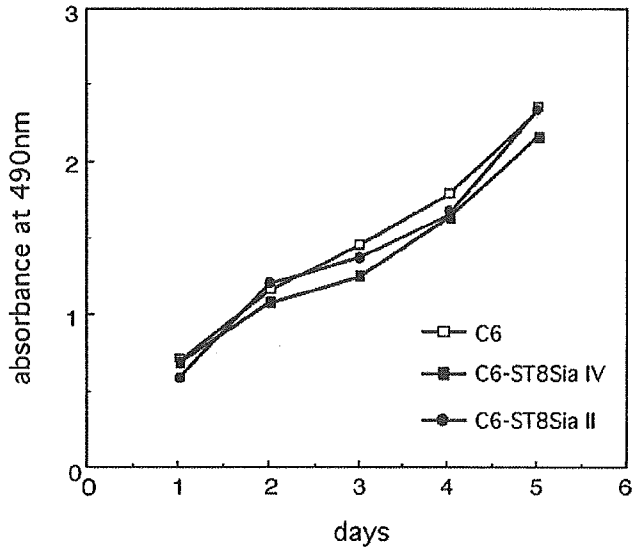

Fig. 4. Comparison of C6 glioma cell growth in vitro. In vitro growth kinetics of the mock-transfected C6, C6-ST8Sia IV, and C6-ST8Sia II cells are shown.

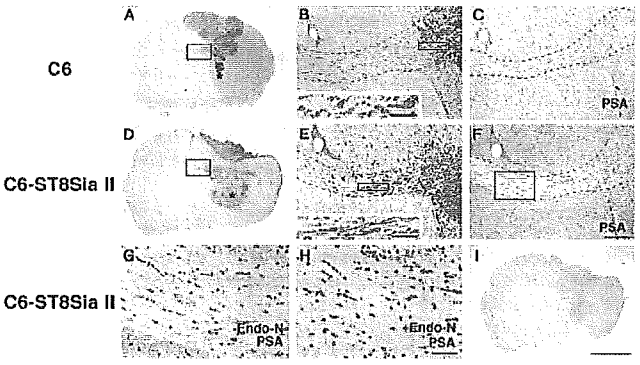

Fig. 5. Invasion of the inoculated C6 glioma cells expressing polysialic acid (PSA) to the corpus callosum of the mice brain. The mock-transfected C6 glioma (**A–C**) and C6-ST8Sia II (**D–I**) cells were injected into the caudate putamen of the brain. Twenty-one days after inoculation, coronal sections of the brain were stained by anti-vimentin antibody (**A, B, D, E**) and anti-PSA antibody, 5A5 (**C, F, G, H**). Digestion with endoneuraminidase-*N* (endo-*N*) was performed before the immunostaining with 5A5 antibody (**H**). Panels **A, D,** and **I** are in the same magnification (bar = 2 mM). Panels **B** and **E** are enlarged figures shown in the box of panels **A** and **D**, respectively, whereas panels **C** and **F** were stained for PSA that are parallel sections of panels **B** and **E** (bar = 200 μm). Inserts in panels **B** and **E** are enlarged figures shown in the box of panels **B** and **E**, respectively (bar = 50 μm). Panels **G** and **H** are enlarged figures shown in the box of panel **F** (bar = 50 μm). Panel **I** indicates a negative control omitting the primary antibodies from the procedure, and no specific staining was found. Envision$^+$ (DAKO) was used for secondary antibody. Counterstaining was performed by hematoxylin. The corpus callosum region and the injected site are shown by dotted lines and a star, respectively.

characteristics in glioma progression. This observation is similar to the fact that axons of the corpus callosum express detectable amounts of PSA on NCAM extending in myelin sheath (Seki and Arai, 1991). To determine whether invasion

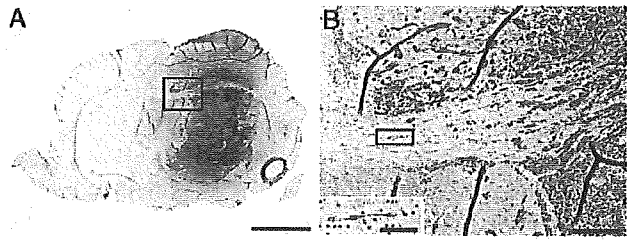

Fig. 6. Invasion to the corpus callosum by C6-ST8Sia IV cells. The invasion assay was carried out in the same way as described in Figure 5. The insert in panel **B** is the enlarged figure indicated in the box of panel **B**, showing extended C6 glioma cells. Bar = 2 mM in panel **A**, 200 μm in panel **B**, and 50 μm in panel **B** insert.

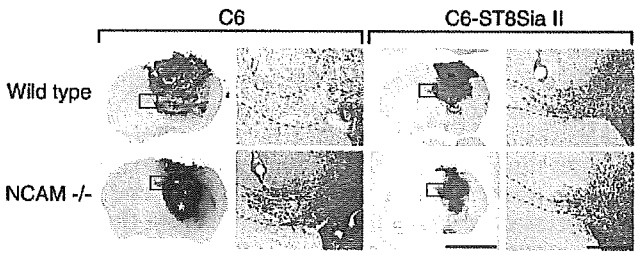

Fig. 7. Invasion of the inoculated C6 glioma cells in the brain of wild type and neural cell adhesion molecule (NCAM)-deficient mice. The mock-transfected C6 glioma and C6-ST8Sia II cells were inoculated into the brain of wild type and NCAM-deficient (NCAM-/-) mice, and the brain was examined in the same way as shown in Figure 5. Right panel (bar = 200 μm) of each set is the enlarged picture of the box in left panel (bar = 2 mm). Immunodetection of vimentin was carried out by using Ventana ES automated DAB immunohistochemical system (Ventana Medical Systems).

by C6 cells is attenuated by PSA-free NCAM–NCAM interaction, we inoculated C6 and C6-ST8Sia II cells into the brain of NCAM-deficient mice. Figure 7 shows that both C6 and C6-ST8Sia II cells invaded into the corpus callosum in NCAM-deficient mice. The results indicate that NCAM–NCAM interaction may prevent C6 cells from invading the corpus callosum in wild-type mice brain, and C6 cells lacking PSA can also invade into the corpus callosum in the absence of NCAM in the host animal.

Discussion

This study demonstrated that glioma cells from patients with astrocytoma express PSA. The frequency of PSA expression was highest in diffuse astrocytoma, which spread extensively, and was apparently associated with recurrence of the disease. We have also revealed that in a patient with recurred diffuse astrocytoma associated with the invasion of corpus callosum, both ST8Sia IV and ST8Sia II confer the expression of PSA on the tumor cells. In previous studies, the overexpression of ST8Sia II has been correlated to the progression of nonsmall cell lung carcinoma (Tanaka *et al.*, 2000). This study expanded these findings to glioma, showing that PSA formed mainly by

ST8Sia IV is associated with the invasive character of glioma cells.

This study also provides direct evidence, for the first time, that PSA plays a role in tumor invasion in the brain. Because glioma tumors rarely metastasize extracranially, we assayed tumor formation inside the brain. C6 glioma cells became highly invasive to the corpus callosum by the acquisition of PSA through the transfection of ST8Sia II or ST8Sia IV. The results strongly suggest that polysialylation facilitates tumor migration. PSA in the transfected C6 glioma cells was shown to attach mostly to the 140-kDa transmembrane NCAM isoform (NCAM-140). Similarly, NCAM-140, but not NCAM-120, is polysialylated in differentiated C2C12 cells (Suzuki *et al.*, 2003). It has been shown that the loss of NCAM-induced metastatic dissemination of pancreatic β cell tumors was observed when β cell tumor-bearing transgenic mice was crossbred with NCAM knockout mice (Perl *et al.*, 1999). This phenotype was reversed by introducing wild-type NCAM-120. These results indicate that PSA attached to NCAM-140 facilitates cell migration. NCAM-140 contains a transmembrane domain, which is absent in NCAM-120. It is tempting to speculate that enhancing glioma invasion may require signal transduction transmitted directly from the extracellular to cytoplasmic domains of NCAM-140. By using TE671 cells that express significant amount of PSA, it has been shown that intraperitoneal injection of TE671 produced lung and liver metastasis. Repeated injection of endo-*N* to remove PSA resulted in the diminishment of lung or liver metastasis (Daniel *et al.*, 2001). Moreover, when metastases occurred in endo-*N*-injected animals, they strongly expressed polysialylated NCAM, which escaped from endo-*N* treatment. These results combined with the results obtained in this study indicate that the expression of PSA leads to increased migration, resulting in increased metastasis.

C6 glioma cells represent a well-differentiated astrocytoma (Thorsen and Tysnes, 1997). After inoculation to the caudate putamen, C6 glioma cells migrated toward the cerebrum cortex and formed tumors in the caudate putamen and cerebrum. Interestingly, PSA-expressing C6 cells invaded the corpus callosum as found in a recurred patient of diffuse astrocytoma. By contrast, such invasion to the corpus callosum was rarely found in the PSA-negative C6 cells. Similarly, PSA expression was more frequently associated with diffuse astrocytoma in the patients examined, suggesting PSA might facilitate cell migration of astrocytoma. The corpus callosum consists of myelinated fibers crossing two hemispheres of the brain. This study also suggests that polysialylated NCAM may weakly interact with adhesive molecules in the corpus callosum (Seki and Arai, 1991), thus allowing cells to migrate in the corpus callosum as shown in previous studies for other systems (Ono *et al.*, 1994; Chazal *et al.*, 2000).

These results, as a whole, indicate that NCAM–NCAM interaction may prevent C6 cells that do not express PSA from migrating into the corpus callosum. It is likely that polysialylation attenuates NCAM–NCAM interaction and facilitates the invasion of polysialylated C6 cells into the corpus callosum. It has also been reported that NCAM may facilitate axonal growth by the stimulation of fibroblast growth factor receptor (Saffell *et al.*, 1997). Similarly, polysialylated NCAM stimulates the signaling by brain-derived neutrophil factor (BDNF), most likely because polysialylated NCAM accumulates BDNF, and presents it to its receptor (Muller *et al.*, 2000; Vutskits *et al.*, 2001; Zhang *et al.*, 2004). Further studies will be necessary to determine if any of those mechanism play a role in glioma invasion facilitated by PSA.

Materials and methods

Tissue collection

Tissue blocks of the primary astrocytomas resected from 44 patients were retrieved from the archives of Shinshu University Hospital, Matsumoto, Japan. According to the World Health Organization (WHO) classification of astrocytic tumors (Kleihuses and Cavenee, 2000), they were categorized into four subtypes, that is, pilocytic astrocytoma (six cases), diffuse astrocytoma (15 cases), anaplastic astrocytoma (16 cases), and glioblastoma multiforme (seven cases). These tissue specimens were fixed for 48 h in 20% buffered formalin (pH 7.4), embedded in paraffin, and sectioned at 4 and 7 μm thickness for immunohistochemistry and in situ hybridization, respectively, as described previously (Machida *et al.*, 2001). The Ethical Committee of Shinshu University School of Medicine approved the protocols for this study.

Immunohistochemistry and in situ hybridization

Immunohistochemical detection of PSA and NCAM was performed by using mouse monoclonal antibodies, 5A5 (mouse IgM, University of Iowa Hybridoma Bank, Iowa City, IA) and 123C3 (mouse IgG_1, Zymed, Carlsbad, CA), respectively. For the NCAM immunostaining, microwave irradiation in a 1.0 mM ethylenediamine tetra-acetic acid (EDTA)–NaOH solution (pH 8.0) was carried out before the incubation with 123C3 antibody, as described previously (Kim *et al.*, 2002). For secondary antibody, Envision$^+$ (DAKO, Glostrup, Denmark), which is dextran polymers conjugating a large number of goat antibodies against mouse immunoglobulins and horseradish peroxidase, was used to increase the sensitivity of immunodetection (Sabattini *et al.*, 1998). The counterstaining was performed with hematoxylin. In control experiments, the primary antibodies were omitted from the staining procedure, and for the PSA staining, pretreatment with endo-*N* that cleaves PSA (Hallenbeck *et al.*, 1987) was also carried out. In these controls, no specific staining was noted.

To construct RNA probes for in situ hybridization, we amplified the ST8Sia IV-specific region (nucleotides –47 to +113; the first nucleotide of the initiation codon is +1) by polymerase chain reaction (PCR) using a primer set of 5′-GCTCTAGAAGGTGCGGGAGCTGG-3′ and 5′-GGGGTACCGATGAGTTGCGTCTCCT-3′. Similarly, the STX-specific region (nucleotides +1 to +138) was amplified by using primers 5′-GCTCTAGATGCAGCTGCAGTTCCGGA-3′ and 5′-GGGGTACCGTTCACAGCTGATCTGATTGT-3′. In these primers, the XbaI and Asp718 sites are underlined. These cDNAs were cloned into the XbaI and Asp718 sites of pGEM-3Zf (+) (Promega, Madison, WI), and the resultant vectors were used as a template for the

construction of the RNA probes, as described previously (Angata *et al.*, 1997; Yeh *et al.*, 2001).

Transfection of C6 glioma cell line with ST8Sia II or ST8Sia IV cDNA vector

pcDNAI-ST8Sia II and pcDNAI-ST8Sia IV harboring cDNA encoding a full-length human ST8Sia II and ST8Sia IV were cloned, as described previously (Nakayama *et al.*, 1995; Angata *et al.*, 1997). The cDNA inserts of pcDNAI-ST8Sia II and pcDNAI-ST8Sia IV were excised by HindIII–XhoI and HindIII–XbaI, respectively, and cloned into corresponding sites of pcDNA3 (Invitrogen, Carlsbad, CA) resulting in pcDNA3-ST8Sia II and pcDNA3-ST8Sia IV.

A rat C6 glioma cell line was transfected with pcDNA3-ST8Sia II or pcDNA3-ST8Sia IV and selected by G418. Clonal cells expressing PSA were chosen after staining with 12F8 anti-PSA antibody (BD Biosciences, San Diego, CA), as described previously (Angata *et al.*, 1997). These cells were designated as C6-ST8Sia II and C6-ST8Sia IV. C6 cells were also transfected with pcDNA3 that lacks cDNA insert, and a cell line isolated after selection with G418 was named mock-transfected C6 cells, C6. These cells were subjected to FACS analysis, as described before (Ohyama *et al.*, 1999).

Western blot analysis

C6, C6-ST8Sia II, and C6-ST8Sia IV cells were subjected to western blot analysis, as described previously (Angata *et al.*, 1997). A portion of cell pellet was digested with endo-*N*. The proteins were separated by sodium dodecyl sulfate–polyacrylamide gel electrophoresis (SDS–PAGE) (6%) and subjected to western blotting using anti-PSA (12F8) or anti-NCAM (5B8) antibody followed by peroxidase-conjugated goat IgG specific to rat IgM or mouse IgG and ECL Plus kit (Amersham Biotech, Piscatany, NJ). HeLa cells expressing NCAM-140 (Nakayama *et al.*, 1995) were used as a positive control.

Cell proliferation assay

C6, C6-ST8Sia II, and C6-ST8Sia IV were seeded in 96-well plates at 10^5 cells/mL in α-MEM Earle's Salts (Irvine Scientific, Santa Ana, CA) containing 10% fetal bovine serum and cultured for various periods. The number of living cells was measured each day by using CellTiter 96® AQueous One Solution Cell Proliferation Assay (Promega), as described previously (Ohyama *et al.*, 1999).

Implantation of C6 cells in mice brain

C6 tumor cells were inoculated into the caudate putamen of adult C57Bl/6 mice, as described previously (Kaye *et al.*, 1986; Chicoine and Silbergeld, 1995). After anesthetizing with tribromoethanol (0.015 mL/g body weight by intraperitoneal injection), C57Bl/6 mice (7- to 9-week-old males, 8 mice for each group of experiments) were set on a stereotaxis frame, and a 1 cm incision was made in the left frontal region of the head. A craniotomy was performed by using a 2-mm bit on a dental drill, and the dura was punctured with a 25-gauge needle. C6 glioma cell suspension [4.8×10^4 cells in 4 μL phosphate-buffered saline (PBS)] was injected by using a Hamilton syringe with a cone-tipped needle attached to the stereotactic frame. Injection was made into the left caudate putamen of the animal at 0.7 mm anterior to the bregma, at 1.8 mm lateral to the midline, and at a depth of 3.0 mm into the brain.

After surgery, the animals were allowed to recover under observation and then returned to their cage. Twenty-one days after surgery, the animals were sacrificed, and brain specimens were prepared for histological analysis. Under the same conditions, C6 and C6-ST8Sia II were inoculated into the brain of mutant mice deficient in NCAM (Cremer *et al.*, 1994) obtained from the Jackson Laboratory (Bar Harbor, ME). NCAM-deficient mice were backcrossed with C57BL/6 mice three generations before use.

Examination of the brain tissue from mice

The mice were deeply anesthetized with tribromoethanol, followed by perfusion with PBS, pH 7.3, and then with 50 mL of 4% paraformaldehyde, 0.2% glutaraldehyde, and 1 mM $MgCl_2$ in 0.1 M sodium phosphate buffer (pH 7.3). Each mouse brain was postfixed in 2% paraformaldehyde, 0.2% glutaraldehyde, and 1 mM $MgCl_2$ in 0.1 M sodium phosphate buffer (pH 7.3) at 4°C overnight. Fixed specimens were embedded in paraffin and cut at 4 μm thickness. Because our preliminary experiments revealed that an intermediate filament, vimentin, which could be detected in astrocytoma (Cosgrove *et al.*, 1989), was strongly expressed in C6 glioma cells (data not shown), the mouse tissue sections were stained with each of two mouse monoclonal antibodies, 5A5 for PSA and V9 mouse IgG_1 (DAKO) for vimentin, followed by treatment with Envision$^+$ (DAKO), as described above, or Ventana ES automated DAB immunohistochemical system (Ventana Medical Systems, Tucson, AZ) (Hayama *et al.*, 2002). The V9 antibody was developed by immunizing swine vimentin and cross-reacts with human, rat, and chicken vimentins. For vimentin staining, microwave irradiation for 25 min in 0.05 M Tris buffer (pH 8.8) containing 1.0 mM EDTA was carried out. In control experiments, primary antibodies were omitted from the staining procedure, and only Envision$^+$ or Ventana system was applied onto the tissue sections. Counterstaining was performed with hematoxylin.

Acknowledgments

We thank Dr. Nobuyoshi Hiraoka for useful discussion, Dr. Edgar Ong for critical reading of the article, and Ms. Aleli Morse for organizing the article. The work was supported by grants R01 CA33895 (to M.F.) and R01 NS41332 (to Y.Y.) awarded by the National Institutes of Health and by grants-in-aid for Scientific Research from the Ministry of Education, Culture, Sports, Science and Technology of Japan (Priority Area 14082201) and the Ministry of Health, Labor and Welfare of Japan (3rd Term Comprehensive Control Research for Cancer) (to J.N.).

Abbreviations

Endo-*N*, endoneuraminidase-*N*; NCAM, neural cell adhesion molecule; PBS, phosphate-buffered saline; PSA, polysialic

acid; ST8Sia II, α2,8-sialyltransferase II; ST8Sia IV, α2,8-sialyltransferase IV.

References

Angata, K., Nakayama, J., Fredette, B., Chong, K., Ranscht, B., and Fukuda, M. (1997) Human STX polysialyltransferase forms the embryonic form of the neural cell adhesion molecule. Tissue-specific expression, neurite outgrowth, and chromosomal localization in comparison with another polysialyltransferase, PST. *J. Biol. Chem.*, **272**, 7182–7190.

Angata, K., Suzuki, M., and Fukuda, M. (1998) Differential and cooperative polysialylation of the neural cell adhesion molecule by two polysialyltransferases, PST and STX. *J. Biol. Chem.*, **273**, 28524–28532.

Angata, K., Suzuki, M., McAuliffe, J., Ding, Y., Hindsgaul, O., and Fukuda, M. (2000) Differential biosynthesis of polysialic acid on neural cell adhesion molecule (NCAM) and oligosaccharide acceptors by three distinct α 2,8-sialyltransferases, ST8Sia IV (PST), ST8Sia II (STX), and ST8Sia III. *J. Biol. Chem.*, **275**, 18594–18601.

Angata, K., Long, J.M., Bukalo, O., Lee, W., Dityatev, A., Wynshaw-Boris, A., Schachner, M., Fukuda, M., and Marth, J.D. (2004) Sialyltransferase ST8Sia-II assembles a subset of polysialic acid that directs hippocampal axonal targeting and promotes fear behavior. *J. Biol. Chem.*, **279**, 32603–32613.

Chazal, G., Durbec, P., Jankovski, A., Rougon, G., and Cremer, H. (2000) Consequences of neural cell adhesion molecule deficiency on cell migration in the rostral migratory stream of the mouse. *J. Neurosci.*, **20**, 1446–1457.

Chicoine, M.R. and Silbergeld, D.L. (1995) Invading C6 glioma cells maintaining tumorigenicity. *J. Neurosurg.*, **83**, 665–671.

Cosgrove, M., Fitzgibbons, P.L., Sherrod, A., Chandrasoma, P.T., and Martin, S.E. (1989) Intermediate filament expression in astrocytic neoplasms. *Am. J. Surg. Pathol.*, **13**, 141–145.

Cremer, H., Lange, R., Christoph, A., Plomann, M., Vopper, G., Roes, J., Brown, R., Baldwin, S., Kraemer, P., Scheff, S., and others. (1994) Inactivation of the N-CAM gene in mice results in size reduction of the olfactory bulb and deficits in spatial learning. *Nature*, **367**, 455–459.

Daniel, L., Durbec, P., Gautherot, E., Rouvier, E., Rougon, G., and Figarella-Branger, D. (2001) A nude mice model of human rhabdomyosarcoma lung metastases for evaluating the role of polysialic acids in the metastatic process. *Oncogene*, **20**, 997–1004.

Eckhardt, M., Muhlenhoff, M., Bethe, A., Koopman, J., Frosch, M., and Gerardy-Schahn, R. (1995) Molecular characterization of eukaryotic polysialyltransferase-1. *Nature*, **373**, 715–718.

Eckhardt, M., Bukalo, O., Chazal, G., Wang, L., Goridis, C., Schachner, M., Gerardy-Schahn, R., Cremer, H., and Dityatev, A. (2000) Mice deficient in the polysialyltransferase ST8SiaIV/PST-1 allow discrimination of the roles of neural cell adhesion molecule protein and polysialic acid in neural development and synaptic plasticity. *J. Neurosci.*, **20**, 5234–5244.

Edelman, G.M. (1984) Modulation of cell adhesion during induction, histogenesis, and perinatal development of the nervous system. *Annu. Rev. Neurosci.*, **7**, 339–377.

Edvardsen, K., Pedersen, P.H., Bjerkvig, R., Hermann, G.G., Zeuthen, J., Laerum, O.D., Walsh, F.S., and Bock, E. (1994) Transfection of glioma cells with the neural-cell adhesion molecule NCAM: effect on glioma-cell invasion and growth *in vivo*. *Int. J. Cancer*, **58**, 116–122.

Finne, J. (1982) Occurrence of unique polysialosyl carbohydrate units in glycoproteins of developing brain. *J. Biol. Chem.*, **257**, 11966–11970.

Fukuda, M. (1996) Possible roles of tumor-associated carbohydrate antigens. *Cancer Res.*, **56**, 2237–2244.

Hallenbeck, P.C., Vimr, E.R., Yu, F., Bassler, B., and Troy, F.A. (1987) Purification and properties of a bacteriophage-induced endo-*N*-acetylneuraminidase specific for poly-α-2,8-sialosyl carbohydrate units. *J. Biol. Chem.*, **262**, 3553–3561.

Hayama, M., Ota, H., Toki, T., Ishii, K., Honda, T., Momose, M., and Nakata, R. (2002) Cell kinetic study of the endometrium by nonisotopic in situ hybridization for histone H3 messenger RNA and immunohistochemistry for Ki-67 and for estrogen and progesterone receptors. *Anat. Rec.*, **266**, 234–240.

Hildebrandt, H., Becker, C., Murau, M., Gerardy-Schahn, R., and Rahmann, H. (1998a) Heterogeneous expression of the polysialyltransferases ST8Sia II and ST8Sia IV during postnatal rat brain development. *J. Neurochem.*, **71**, 2339–2348.

Hildebrandt, H., Becker, C., Gluer, S., Rosner, H., Gerardy-Schahn, R., and Rahmann, H. (1998b) Polysialic acid on the neural cell adhesion molecule correlates with expression of polysialyltransferases and promotes neuroblastoma cell growth. *Cancer Res.*, **58**, 779–784.

Kaye, A.H., Morstyn, G., Gardner, I., and Pyke, K. (1986) Development of a xenograft glioma model in mouse brain. *Cancer Res.*, **46**, 1367–1373.

Kim, W.J., Terada, N., Nomura, T., Takahashi, R., Lee, S.D., Park, J.H., and Konno, A. (2002) Effect of formaldehyde on the expression of adhesion molecules in nasal microvascular endothelial cells: the role of formaldehyde in the pathogenesis of sick building syndrome. *Clin. Exp. Allergy*, **32**, 287–295.

Kiss, J.Z. and Rougon, G. (1997) Cell biology of polysialic acid. *Curr. Opin. Neurobiol.*, **7**, 640–646.

Kleene, R. and Schachner, M. (2004) Glycans and neural cell interactions. *Nat. Rev. Neurosci.*, **5**, 195–208.

Kleihuses, P. and Cavenee, W.K. (2000) *Pathology and Genetics of Tumors of the Nervous System*. IARC Press, Lyon.

Livingston, B.D. and Paulson, J.C. (1993) Polymerase chain reaction cloning of a developmentally regulated member of the sialyltransferase gene family. *J. Biol. Chem.*, **268**, 11504–11507.

Machida, E., Nakayama, J., Amano, J., and Fukuda, M. (2001) Clinicopathological significance of core 2 β1,6-*N*-acetylglucosaminyltransferase messenger RNA expressed in the pulmonary adenocarcinoma determined by in situ hybridization. *Cancer Res.*, **61**, 2226–2231.

Martersteck, C.M., Kedersha, N.L., Drapp, D.A., Tsui, T.G., and Colley, K.J. (1996) Unique α 2, 8-polysialylated glycoproteins in breast cancer and leukemia cells. *Glycobiology*, **6**, 289–301.

Muller, D., Djebbara-Hannas, Z., Jourdain, P., Vutskits, L., Durbec, P., Rougon, G., and Kiss, J.Z. (2000) Brain-derived neurotrophic factor restores long-term potentiation in polysialic acid-neural cell adhesion molecule-deficient hippocampus. *Proc. Natl. Acad. Sci. U S A.*, **97**, 4315–4320.

Nakayama, J., Fukuda, M.N., Fredette, B., Ranscht, B., and Fukuda, M. (1995) Expression cloning of a human polysialyltransferase that forms the polysialylated neural cell adhesion molecule present in embryonic brain. *Proc. Natl. Acad. Sci. U S A.*, **92**, 7031–7035.

Ohyama, C., Tsuboi, S., and Fukuda, M. (1999) Dual roles of sialyl Lewis X oligosaccharides in tumor metastasis and rejection by natural killer cells. *EMBO J.*, **18**, 1516–1525.

Ong, E., Nakayama, J., Angata, K., Reyes, L., Katsuyama, T., Arai, Y., and Fukuda, M. (1998) Developmental regulation of polysialic acid synthesis in mouse directed by two polysialyltransferases, PST and STX. *Glycobiology*, **8**, 415–424.

Ono, K., Tomasiewicz, H., Magnuson, T., and Rutishauser, U. (1994) N-CAM mutation inhibits tangential neuronal migration and is phenocopied by enzymatic removal of polysialic acid. *Neuron*, **13**, 595–609.

Owens, G.C., Orr, E.A., DeMasters, B.K., Muschel, R.J., Berens, M.E., and Kruse, C.A. (1998) Overexpression of a transmembrane isoform of neural cell adhesion molecule alters the invasiveness of rat CNS-1 glioma. *Cancer Res.*, **58**, 2020–2028.

Perl, A.K., Dahl, U., Wilgenbus, P., Cremer, H., Semb, H., and Christofori, G. (1999) Reduced expression of neural cell adhesion molecule induces metastatic dissemination of pancreatic beta tumor cells. *Nat. Med.*, **5**, 286–291.

Roth, J., Zuber, C., Wagner, P., Taatjes, D.J., Weisgerber, C., and Heitz, P.U. (1988) Reexpression of poly (sialic acid) units of the neural cell adhesion molecule in Wilms tumor. *Proc. Natl. Acad. Sci. U S A.*, **85**, 2999–3003.

Rutishauser, U. and Landmesser, L. (1996) Polysialic acid in the vertebrate nervous system: a promoter of plasticity in cell–cell interactions. *Trends Neurosci.*, **19**, 422–427.

Sabattini, E., Bisgaard, K., Ascani, S., Poggi, S., Piccioli, M., Ceccarelli, C., Pieri, F., Fraternali-Orcioni, G., and Pileri, S.A. (1998) The EnVision++ system: a new immunohistochemical method for diagnostics and research. Critical comparison with the APAAP, ChemMate, CSA, LABC, and SABC techniques. *J. Clin. Pathol.*, **51**, 506–511.

Saffell, J.L., Williams, E.J., Mason, I.J., Walsh, F.S., and Doherty, P. (1997) Expression of a dominant negative FGF receptor inhibits

axonal growth and FGF receptor phosphorylation stimulated by CAMs. *Neuron*, **18**, 231–242.

Scheidegger, E.P., Lackie, P.M., Papay, J., and Rothm, J. (1994) *In vitro* and *in vivo* growth of clonal sublines of human small cell lung carcinoma is modulated by polysialic acid of the neural cell adhesion molecule. *Lab. Invest.*, **70**, 95–106.

Scheidegger, E.P., Sternberg, L.R., Roth, J., and Lowe, J.B. (1995) A human STX cDNA confers polysialic acid expression in mammalian cells. *J. Biol. Chem.*, **270**, 22685–22688.

Seidenfaden, R., Gerardy-Schahn, R., and Hildebrandt, H. (2000) Control of NCAM polysialylation by the differential expression of polysialyltransferases ST8SiaII and ST8SiaIV. *Eur. J. Cell Biol.*, **79**, 680–688.

Seki, T. and Arai, Y. (1991) Expression of highly polysialylated NCAM in the neocortex and piriform cortex of the developing and the adult rat. *Anat. Embryol. (Berl)*, **184**, 395–401.

Smith, S.R., Auerbach, B., and Morgan, L. (1996) Serum neural cell adhesion molecule in multiple myeloma and other plasma cell disorders. *Br. J. Haematol.*, **92**, 67–70.

Suzuki, M., Angata, K., Nakayama, J., and Fukuda, M. (2003) Polysialic acid and mucin type *O*-glycans on the neural cell adhesion molecule differentially regulate myoblast fusion. *J. Biol. Chem.*, **278**, 49459–49468.

Tanaka, F., Otake, Y., Nakagawa, T., Kawano, Y., Miyahara, R., Li, M., Yanagihara, K., Nakayama, J., Fujimoto, I., Ikenaka, K., and Wada, H. (2000) Expression of polysialic acid and STX, a human polysialyltransferase, is correlated with tumor progression in non-small cell lung cancer. *Cancer Res.*, **60**, 3072–3080.

Thorsen, F. and Tysnes, B.B. (1997) Brain tumor cell invasion, anatomical and biological considerations. *Anticancer Res.*, **17**, 4121–4126.

Van Camp, B., Durie, B.G., Spier, C., De Waele, M., Van Riet, I., Vela, E., Frutiger, Y., Richter, L., and Grogan, T.M. (1990) Plasma cells in multiple myeloma express a natural killer cell-associated antigen: CD56 (NKH-1; Leu-19). *Blood*, **76**, 377–382.

Vutskits, L., Djebbara-Hannas, Z., Zhang, H., Paccaud, J.P., Durbec, P., Rougon, G., Muller, D., and Kiss, J.Z. (2001) PSA-NCAM modulates BDNF-dependent survival and differentiation of cortical neurons. *Eur. J. Neurosci.*, **13**, 1391–1402.

Yamaguchi, Y. (2000) Lecticans: organizers of the brain extracellular matrix. *Cell. Mol. Life Sci.*, **57**, 276–289.

Yeh, J.C., Hiraoka, N., Petryniak, B., Nakayama, J., Ellies, L.G., Rabuka, D., Hindsgaul, O., Marth, J.D., Lowe, J.B., and Fukuda, M. (2001) Novel sulfated lymphocyte homing receptors and their control by a Corel extension β 1,3-*N*-acetylglucosaminyltransferase. *Cell*, **105**, 957–969.

Yoshida, Y., Kojima, N., and Tsuji, S. (1995) Molecular cloning and characterization of a third type of *N*-glycan α2,8-sialyltransferase from mouse lung. *J. Biochem. (Tokyo)*, **118**, 658–664.

Zhang, H., Vutskits, L., Calaora, V., Durbec, P., and Kiss, J.Z. (2004) A role for the polysialic acid-neural cell adhesion molecule in PDGF-induced chemotaxis of oligodendrocyte precursor cells. *J. Cell Sci.*, **117**, 93–103.

0023-6837/03/8302-187$03.00/0
LABORATORY INVESTIGATION

Vol. 83, No. 2, p. 187, 2003
Printed in U.S.A.

Usefulness of the Real-Time Reverse Transcription-Polymerase Chain Reaction Assay Targeted to α1,4-*N*-Acetylglucosaminyltransferase for the Detection of Gastric Cancer

Fumiaki Shimizu, Jun Nakayama, Satoshi Ishizone, Mu Xia Zhang, Masatomo Kawakubo, Hiroyoshi Ota, Atsushi Sugiyama, Seiji Kawasaki, Minoru Fukuda, and Tsutomu Katsuyama

Departments of Laboratory Medicine (FS, JN, SI, MXZ, MK, HO, TK) and Surgery (FS, SI, AS, SK), Shinshu University School of Medicine, Matsumoto, Japan; Institute of Organ Transplants, Reconstructive Medicine, and Tissue Engineering (JN), Shinshu University Graduate School of Medicine and Department of Medical Technology (HO), School of Allied Medical Sciences, Shinshu University, Matsumoto, Japan; and Glycobiology Program (MF), the Burnham Institute, La Jolla, California

SUMMARY: α1,4-*N*-acetylglucosaminyltransferase (α4GnT) is a glycosyltransferase that forms a unique glycan, GlcNAcα1→4Galβ→R, specifically present in gastric gland mucous cell-type mucin. Recently, we molecularly cloned human α4GnT and showed that α4GnT is expressed in the mucous cells that secrete this particular mucin. In the present study, we first demonstrated that α4GnT was frequently expressed in gastric cancer cells but not in peripheral blood cells using immunohistochemistry. To detect gastric cancer cells circulating in the peripheral blood of gastric cancer patients, we quantitatively analyzed the expression level of α4GnT mRNA in the mononuclear cell fraction of peripheral blood using real-time reverse transcription polymerase chain reaction. The transcripts of α4GnT were detected in the mononuclear cell fraction isolated from 62.2% of 37 gastric cancer patients but not from any of 23 healthy individuals. Significant correlation was found in the expression levels of α4GnT mRNA in peripheral blood and α4GnT protein in gastric cancer cells. Surprisingly, α4GnT mRNA was detectable in 80% of five patients with an early stage of gastric cancer when the cancer cells were limited to the gastric mucosa, and the expression levels of α4GnT mRNA were increased in association with tumor progression. In three patients with gastric cancer, during postsurgical follow-up, the expression levels of α4GnT mRNA were decreased after surgical removal of gastric cancer. However, significant amounts of the α4GnT transcripts were again detected in two patients, who eventually developed to the recurrence of gastric cancer. Although α4GnT was detected in 33.3% of nine patients with *Helicobacter pylori*–infected chronic active gastritis as well as all of four patients with peptic ulcer, the mean expression level of α4GnT mRNA in these benign disorders was lower than that in gastric cancer. These results altogether indicate that the quantitative analysis of α4GnT mRNA expressed in the peripheral blood is useful for the detection and, possibly, monitoring of gastric cancer. (*Lab Invest 2003, 83:187–197*).

Gastric cancer is the most frequently diagnosed malignancy as well as one of the leading causes of tumor death in both men and women in Japan (Sun et al, 2001). When the gastric cancer is detected in early stages, favorable outcome is expected when the tumor is completely removed by surgical procedure (Patino, 1994). However, it also has been documented that the advanced gastric cancer showing serosal invasion frequently recurred even when the extensive resection of the primary tumor together with lymphadenectomy was performed (Boku et al, 1990; Wanebo et al, 1993). This indicates that the early detection of the gastric cancer is critical to expect favorable outcome of this disease. For the gastric mass screening, the indirect photofluorography or tumor markers such as carcinoembryonic antigen (CEA) and CA19-9 are widely used. However, it has been documented that these methods have limitation in detecting early stages of the gastric cancer when the cancer cells are restricted to the gastric mucosa (Pectasides et al, 1997).

Recently, extensive studies have been carried out to detect circulating gastric cancer cells in the peripheral blood by using the reverse transcription polymerase

DOI: 10.1097/01.LAB.0000057001.21187.A0

Received December 18, 2002.

This work was supported by Grant-in-Aids for Scientific Research on Priority Area 10178104, 14030032, and, in part, 14082201 from the Ministry of Education, Culture, Sports, Science and Technology of Japan (to JN) and by NIH Grant CA48737 from the National Cancer Institute (to MF).

Address reprint requests to: Dr. Jun Nakayama, Department of Pathology, Shinshu University School of Medicine, Asahi 3-1-1, Matsumoto 390-8621, Japan. E-mail: jun@hsp.md.shinshu-u.ac.jp

chain reaction (RT-PCR) method targeted to the specific genes including CEA and cytokeratin 19 (CK19) (Aihara et al, 1997; Majima et al, 2000; Nishida et al, 2000; Piva et al, 2000; Yeh et al, 1998). Although CEA transcripts were detected in the mononuclear cell fraction isolated from approximately 30 to 40% of patients with gastric cancer (Nishida et al, 2000; Piva et al, 2000), Piva et al (2000) reported that CEA mRNA was positive in 1 of 16 control subjects. However, CK19 mRNA was less frequently detected in the peripheral blood compared with CEA, and thus only 9.6 to 20.6% of the patients with gastric cancer were positive for CK19 transcripts (Majima et al, 2000; Yeh et al, 1998). More important, both CEA and CK19 are widely expressed not only in gastric cancer cells but also in other epithelial cell–derived tumor cells such as colorectal and breast cancers. In fact, CEA mRNA was detected in 34% of patients with colorectal cancer (Piva et al, 2000). In addition, transcripts of CK19 and CEA are inducible in hematopoietic cells in the presence of inflammatory cytokines such as interleukin-3 and interferon-γ (Jung et al, 1998). Thus, identification of new molecules much more selectively expressed in gastric cancer cells may be helpful to improve the diagnosis of gastric cancer.

Glycoproteins secreted from the mucous cells such as mucous neck cell and pyloric gland cell of gastric mucosa and Brunner's gland of duodenal mucosa characteristically contain GlcNAcα1→4Galβ→R structures in terminal ends of the oligosaccharides in O-glycans (Ishihara et al, 1996). This unique carbohydrate is frequently expressed in the gastric cancer cells, thus being regarded as a tumor-associated carbohydrate antigen for this particular cancer (Nakamura et al, 1998). By expression cloning, we have recently isolated a cDNA encoding human α1,4-*N*-acetylglucosaminyltransferase (α4GnT), which is responsible for the biosynthesis of GlcNAcα1→4Galβ→R residue (Nakayama et al, 1999). In addition, Northern blot or immunohistochemical analysis using anti-α4GnT antibody demonstrated that this enzyme is found to be exclusively limited to the gastroduodenal mucosa as well as pancreaticobiliary tract showing gastric metaplasia, where GlcNAcα1→4Galβ→R residues are expressed (Nakayama et al, 1999; Zhang et al, 2001). These results as a whole indicate that α4GnT plays a key role in forming GlcNAcα1→4Galβ→R residues in vivo and may be expressed in gastric cancer cells that produce this unique glycan.

In the present study, we first demonstrated that α4GnT is frequently expressed in gastric cancer cells but not in the peripheral blood cells by immunohistochemistry using a specific antibody against α4GnT. Then, we quantitatively measured the expression level of α4GnT mRNA in the mononuclear cell fraction of peripheral blood isolated from gastric cancer patients by using real-time RT-PCR, demonstrating the clinical usefulness of this assay for the detection and monitoring of gastric cancer.

Results

Expression of α4GnT in Gastric Cancer Cells

To determine whether α4GnT was expressed in the gastric cancer cells, we performed immunohistochemistry of the gastric cancer tissues resected from the patients, whose blood samples had been collected before the surgery, using the anti-α4GnT antibody I17K (Zhang et al, 2001). Among the 29 patients examined, α4GnT seemed to be expressed in the Golgi region of gastric cancer cells in 22 patients (75.9%), irrespective of the histopathological classifications of the gastric cancer (Fig. 1, A to C). The same experiments also demonstrated that α4GnT was detected in the mucous neck cells and pyloric glands found in the normal gastric mucosa, as described before (Zhang et al, 2001) (Fig. 1D), and that the peripheral blood cells including leukocytes and lymphocytes were negative for α4GnT (Fig. 1, arrows and arrowheads). These results combined suggested that the RT-PCR method targeted to α4GnT mRNA would be useful to detect the circulating tumor cells in the peripheral blood of patients with gastric cancer, because α4GnT was not expressed in leukocytes and lymphocytes.

Construction of Standard Curve for the Real-Time RT-PCR Assay

The standard curve for α4GnT constructed by using 10-fold dilutions of α4GnT cDNA, pcDNA!-α4GnT, is shown in Figure 2. The cycle number where the fluorescence reached the detection threshold was defined as C_T, and a strong linear relationship between the C_T and the log of the amount of the cDNAs was demonstrated. On the basis of the standard curve, we could detect α4GnT cDNA from 6×10^{-2} to 2.4×10^{-10} μg/ml, corresponding to 1×10^{10} to 4×10^{1} copies/ml. Thus, the amount of α4GnT transcripts more than 40 copies/ml was defined to be positive for the α4GnT. Similarly, the standard curve for a housekeeping gene, glyceraldehyde-3-phosphate dehydrogenase (GAPDH) was constructed by using 10-fold dilutions of pCR2.1-GAPDH ranging from 1.2×10^{-2} to 1.2×10^{-6} μg/ml (data not shown). With the use of these standard curves, amounts of α4GnT mRNA and GAPDH mRNA were determined, and the relative expression level of α4GnT was defined by multiplying α4GnT:GAPDH mRNA ratios by 1.0×10^{7}.

Detection of α4GnT mRNA in Peripheral Blood Samples Derived from Healthy Volunteers and Patients with Helicobacter pylori–Infected Chronic Active Gastritis

By using the real-time RT-PCR, expression of α4GnT mRNA in the mononuclear cell fraction of peripheral blood obtained from the healthy volunteers and patients with *H. pylori*–infected chronic active gastritis as well as patients with peptic gastroduodenal ulcers

was examined (Fig. 3). In 23 healthy volunteers, the transcripts of α4GnT were not detectable in the peripheral blood. With the use of the commercially available blood cell cDNA panels, it was also shown that α4GnT mRNA was not detectable in leukocytes, mononuclear cells (B cells, T cells, and monocytes), resting and activated CD8+ cells, resting and activated CD4+ cells, resting and activated CD19+ cells, resting CD14+ cell, and activated mononuclear cells. In the patients with chronic active gastritis or peptic gastroduodenal ulcer, however, α4GnT transcripts in the peripheral blood were detected in three (33.3%) of nine patients with gastritis and in all of four patients with peptic ulcer. It is interesting that the relative amounts of α4GnT mRNA to GAPDH mRNA in the patients with ulcer was shown to be significantly higher than that in the chronic active gastritis (3.156 ± 0.498 versus 0.406 ± 0.206 [mean ± SE]; $p < 0.05$, Dunnett's test; Fig. 3), indicating that gastric mucous cells expressing α4GnT could enter the peripheral blood stream through mucosal disruption or ulceration, and the relative amount of α4GnT transcripts in the peripheral blood might reflect the extent of the mucosal damage.

Detection of α4GnT mRNA in Peripheral Blood Samples of Patients with Gastric Cancer

To determine whether α4GnT mRNA was detected in the mononuclear cell fraction of peripheral blood taken from patients with gastric cancer, we performed quantitative analysis of α4GnT mRNA for 37 patients with gastric cancer. The transcripts of α4GnT were detected in 23 (62.2%) of the patients with gastric

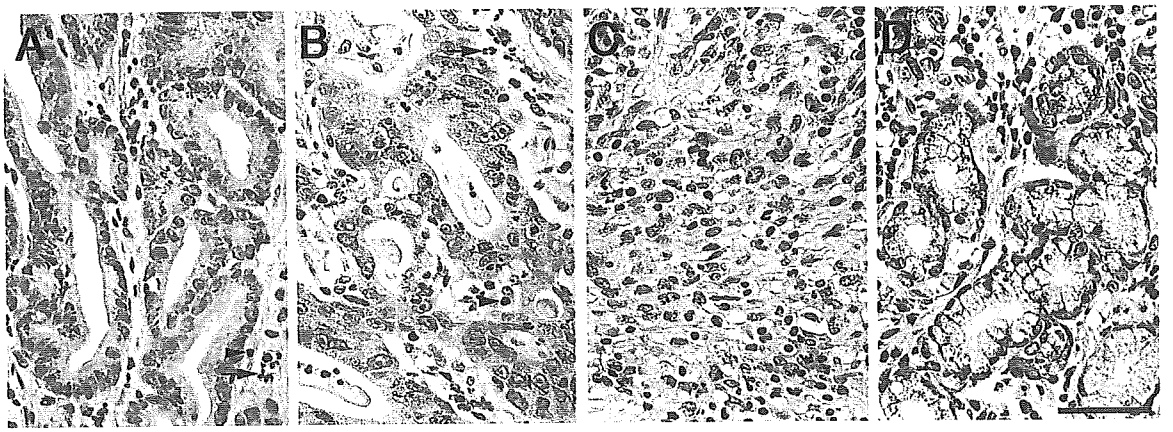

Figure 1.
Immunohistochemical detection of α1,4-*N*-acetylglucosaminyltransferase (α4GnT) protein in gastric cancer cells and normal pyloric gland cells. α4GnT is expressed in the Golgi region of gastric cancer cells of intestinal-type carcinoma (A and B) and diffuse-type carcinoma (C). It is also expressed in the Golgi region of normal pyloric gland cells of the stomach (D). Immunohistochemistry with anti-α4GnT antibody 117K. Arrows and arrowhead indicate leukocytes and lymphocytes, respectively. Bar = 50 μm.

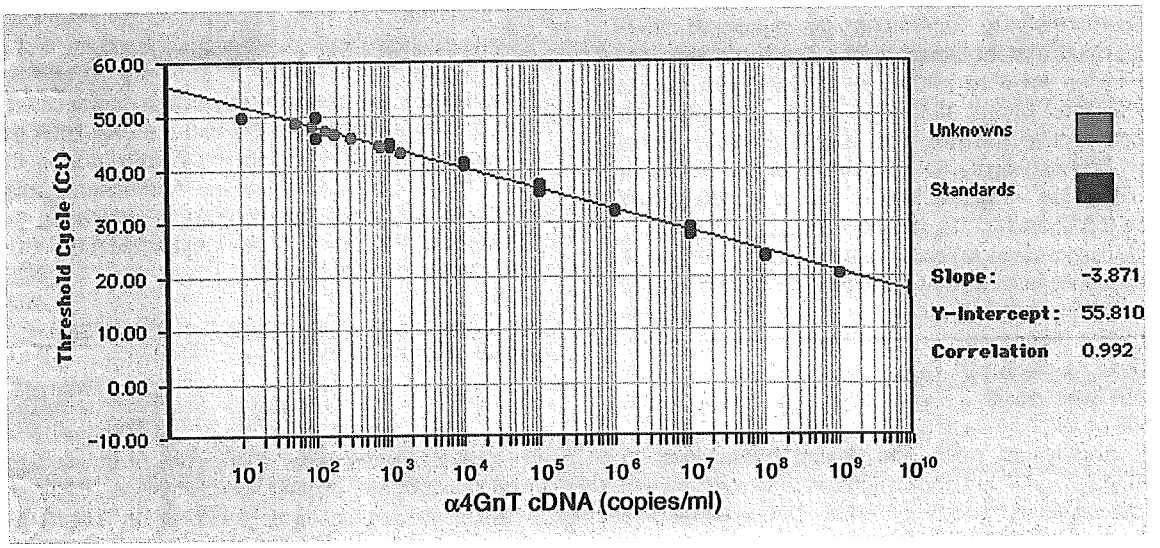

Figure 2.
Standard curve of real-time reverse transcription polymerase chain reaction (RT-PCR) of α4GnT mRNA. A plasmid encoding human α4GnT, pcDNAI-α4GnT, was serially diluted from 10^{10} to 10^{1} copies/ml and used to construct the standard curve (black dots). Unknowns (red dots) represent patients' samples.

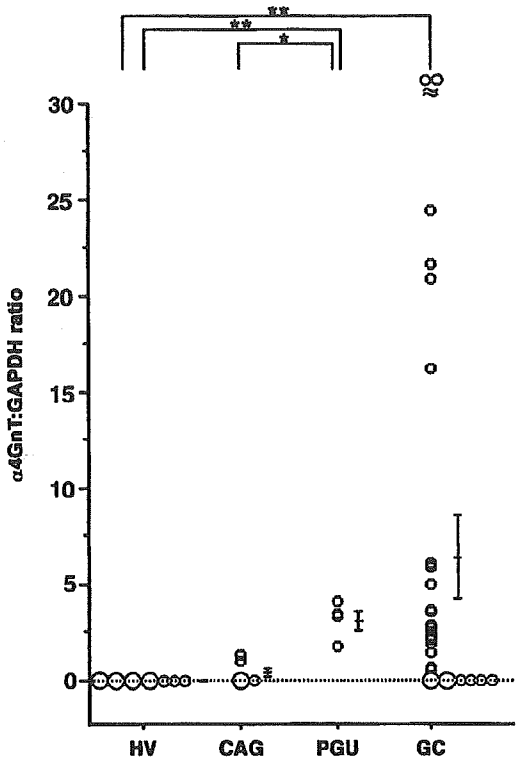

Figure 3.

Expression levels of α4GnT mRNA determined by real-time RT-PCR method in the mononuclear cell fraction of peripheral blood from healthy volunteers and patients with chronic active gastritis, peptic gastroduodenal ulcer, and gastric cancer. Small and large circles indicate one and five people, respectively. α4GnT:glyceraldehyde-3-phosphate dehydrogenase mRNA ratios multiplied by 1.0×10^7 are indicated, and bars indicate mean ± SE. HV, healthy volunteers; CAG, chronic active gastritis; PGU, peptic gastroduodenal ulcer; GC, gastric cancer; $^*p < 0.05$; $^{**}p < 0.01$ (Dunnett's test).

cancer, and the relative expression level of α4GnT mRNA to GAPDH mRNA in the patients with gastric cancer was 6.461 ± 2.164 (mean ± SE), significantly higher than that in the normal volunteer ($p < 0.01$, Dunnett's test; Fig. 3). Although the significant differences were not obtained by the Dunnett's test, the expression level of α4GnT in patients with gastric cancer was higher than that in the patients with chronic active gastritis and peptic gastroduodenal ulcer. The sensitivity and specificity of this assay for the detection of gastric cancer are, thus, determined to be 0.622 and 0.806, respectively.

The expression levels of α4GnT in the peripheral blood taken from the 37 patients with gastric cancer were then evaluated by clinicopathological variables that were determined at the subsequent surgical operation. As shown in Table 1, the amount of α4GnT mRNA was positively correlated with tumor stage, depth of tumor invasion, vessel and lymphatic invasion, and lymph node and distant metastases. In particular, significant correlations were found between the tumor stage I and IV ($p < 0.05$, Dunnett's test) as well as in distant metastasis ($p = 0.0157$, Mann-Whitney *U* test). Regarding the histopathological classification of gastric cancer (Laurén, 1965), the α4GnT transcripts were more abundantly detected in the peripheral blood of patients with diffuse-type carcinoma than in those with intestinal-type carcinoma (Table 1).

In 29 patients with gastric cancer, the expression levels of α4GnT mRNA in peripheral blood were compared with the expression level of α4GnT protein determined by the immunohistochemistry of the subsequently resected stomach using the anti-α4GnT antibody I17K as described above (Fig. 4). The transcripts of α4GnT were more abundantly expressed in the peripheral blood of the patients who were positive for α4GnT protein in the gastric cancer cells compared with the patients who were negative for α4GnT protein in the cancer cells with statistical significance (9.505 ± 3.447 versus 0.696 ± 0.455 [mean ± SE]; $p = 0.0270$, Mann-Whitney *U* test). Taking into account that α4GnT is not detectable in the peripheral blood cells including leukocytes, lymphocytes, and monocytes, these combined results suggest that α4GnT mRNA detected in the peripheral blood of the patients with gastric cancer originated from circulating gastric cancer cells. Thus, the real-time RT-PCR method targeted to α4GnT mRNA would allow us to detect such circulating cancer cells.

Detection of α4GnT mRNA in the Peripheral Blood of the Patients with Gastric Cancer during the Course of Postsurgical Follow-Up

To examine the expression level of α4GnT mRNA during the course of postsurgical follow-up, we analyzed the mononuclear cell fraction of the peripheral blood obtained from three patients with gastric cancer by real-time RT-PCR (Table 2). In all of the patients, α4GnT mRNA detected in the peripheral blood before the operation turned out to be negative after the surgical removal of gastric cancer, irrespective of the stages. In a nonrecurred patient with stage II (patient 21), small amounts of α4GnT mRNA comparable with those in the chronic active gastritis were detected 464 days after the operation. In contrast, the significant amounts of α4GnT mRNA were again detected in the recurred patients with stage III (patients 30 and 31) 372 and 362 days after the operation, respectively. These results indicate that the real-time RT-PCR assay targeted to α4GnT might be helpful during the course of postsurgical follow up. Additional studies with larger series will be required to determine the usefulness of this assay for the postsurgical monitoring of gastric cancer.

Comparison of α4GnT mRNA with Two Distinct Tumor Markers, CEA and CA19-9

The results of the quantitative analysis for α4GnT mRNA in peripheral blood of the preoperative patients with gastric cancer were then compared with the serum levels of two distinct tumor markers, CEA and CA19-9, in the same patients. As shown in Table 3, the expression levels of α4GnT mRNA were not correlated with those of either CEA or CA19-9, irrespective of the tumor stages. In addition, it was shown that the sensitivity of α4GnT for the detection of gastric cancer

Table 1. Correlation of the Expression Level of α4GnT mRNA in the Mononuclear Cell Fraction of Peripheral Blood from Patients with Gastric Cancer with Clinicopathological Variables

	Frequency of positive patients[a]	α4GnT:GAPDH ratio[b] (mean ± SE)	p
Tumor stage			
I	11/19 (57.9%)	1.632 ± 0.492	
II	2/6 (33.3%)	4.073 ± 3.548	<0.05[c]
III	4/6 (66.7%)	14.389 ± 7.249	
IV	6/6 (100%)	16.210 ± 9.614	
Depth of tumor invasion			
Intramucosa	4/5 (80.0%)	1.090 ± 0.560	
Submucosa	6/11 (54.5%)	2.135 ± 0.780	
Proper muscle	2/4 (50.0%)	6.345 ± 5.180	0.8301[d]
Subserosa	4/8 (50.0%)	9.575 ± 5.760	
Serosa	6/8 (75.0%)	13.205 ± 7.525	
Venous invasion			
Negative	12/18 (66.7)	3.117 ± 1.351	0.7942[e]
Positive	10/18 (55.6%)	10.024 ± 4.135	
Lymphatic invasion			
Negative	7/12 (58.3%)	1.760 ± 0.681	0.3778[e]
Positive	15/24 (62.5%)	8.976 ± 3.225	
Lymph node metastasis			
Negative	11/20 (55.0%)	1.662 ± 0.475	0.0850[e]
Positive	11/16 (68.8%)	12.705 ± 4.587	
Distant metastasis			
Negative	17/31 (54.8%)	4.573 ± 1.729	0.0157[e]
Positive	6/6 (100%)	16.211 ± 9.615	
Histopathology[f]			
Intestinal type	15/25 (60.0%)	5.781 ± 1.156	0.3858[e]
Diffuse type	8/12 (66.7%)	20.671 ± 5.967	

[a] The amounts of α4GnT mRNA more than 40 copies/ml in a reaction tube are defined as positive.
[b] α4GnT:GAPDH mRNA ratios multiplied by 1.0×10^7 are indicated.
[c] Analyzed by Dunnett's test. Significant difference was found between stage I and IV.
[d] Analyzed by Kruskal-Wallis test.
[e] Analyzed by Mann-Whitney *U* test.
[f] The Laurén classification.

seemed to be superior to that of CEA and CA19-9, ie, α4GnT was detected in 23 (62.2%) of 37 patients, whereas CEA and CA19-9 were merely detected in 11 (29.7%) and 3 (8.1%) patients, respectively. It is noteworthy that all patients with stage IV were positive for α4GnT transcripts, whereas CEA and CA19-9 were not highly elevated in some of these patients.

Detection of α4GnT mRNA in Peripheral Blood Samples of Patients with Cancer Other Than Gastric Cancer

The expression levels of α4GnT mRNA in mononuclear cell fraction of the peripheral blood taken from patients with cancers other than gastric cancer were also measured by the real-time RT-PCR method. As shown in Table 4, α4GnT mRNA was not detectable in the patients with esophageal cancer, lung cancer, breast cancer, and uterine cancer. Small amounts of α4GnT mRNA comparable with those of chronic active gastritis were detected in two (20%) and one (25%) colorectal and liver cancer patients, respectively. By contrast, significant amounts of α4GnT mRNA comparable with those of gastric cancer were detected in all of the patients with pancreatic cancer and carci-

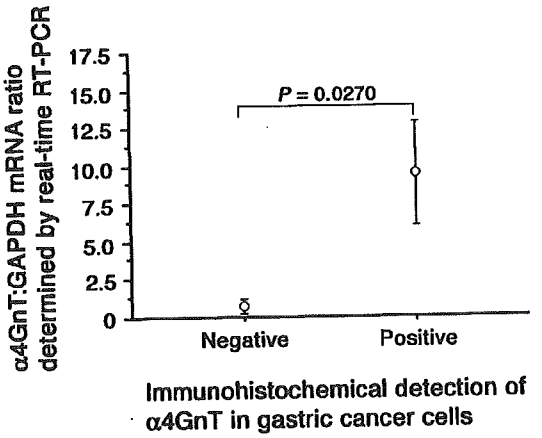

Figure 4.
Correlation of the expression levels of α4GnT mRNA detected in the peripheral blood by real-time RT-PCR and the expression of α4GnT detected by using anti-α4GnT antibody 117K in the subsequently resected gastric cancer. The expression level of α4GnT mRNA detected in the peripheral blood from the patients whose cancer cells express α4GnT is significantly higher than that from the patients whose cancer cells do not express α4GnT ($p = 0.0270$, Mann-Whitney *U* test).

Table 2. Expression Level of α4GnT mRNA in the Mononuclear Cell Fraction of Peripheral Blood from Patients with Gastric Cancer during Postsurgical Follow-up

Patient	Stage	Days post-surgery	α4GnT:GAPDH ratio[a]	Outcome
21	II	−1	21.65	
		1	0	
		7	0	
		10	0	
		21	0	
		464	0.9925	No recurrence
30	III	−4	44.25	
		7	0	
		14	0	
		24	0	
		49	0	
		104	0	
		372	2.636	
		428		Died
31	III	−1	16.215	
		14	0	
		25	0	
		362	7.883	
		485	8.365	
		508		Died

[a] α4GnT:GAPDH mRNA ratios multiplied by 1.0×10^7 are indicated.

Table 3. Comparison of Frequencies of Positive Patients for α4GnT mRNA, CEA, and CA19-9 Detected in Peripheral Blood of Patients with Gastric Cancer

Tumor stage	α4GnT mRNA (> 40 copies/ml)	CEA (> 2.5 ng/ml)	CA19-9 (> 37 U/ml)
I	11/19 (57.9%)	3/19 (15.8%)	0/19 (0%)
II	2/6 (33.3%)	2/6 (33.3%)	0/6 (0%)
III	4/6 (66.7%)	2/6 (33.3%)	0/6 (0%)
IV	6/6 (100%)	4/6 (66.7%)	3/6 (50.0%)
Total	23/37 (62.2%)	11/37 (29.7%)	3/37 (8.1%)

noma of the papilla vater as well as in three (60%) patients with bile duct cancer, suggesting the possible usefulness of this assay for the detection of pancreatic and bile duct cancers as well as papilla vater cancer.

Discussion

α4GnT is a glycosyltransferase responsible for the biosynthesis of GlcNAcα1→4Galβ→R structures characteristic for the gastric gland mucous cell-type mucin (Nakayama, 2002). In the present study, we first demonstrated that this enzyme is frequently expressed in the gastric cancer cells, but not in peripheral blood cells, using immunohistochemistry with a specific antibody for α4GnT, I17K (see Fig. 1). By using real-time RT-PCR targeted to the α4GnT mRNA, we could detect the transcripts of α4GnT in the

Table 4. Detection of α4GnT mRNA by Real-Time RT-PCR Method in the Mononuclear Cell Fraction of Peripheral Blood from Patients with Cancer Other Than Gastric Cancer

Cancer location	Frequency of positive patients[a]	α4GnT:GAPDH ratio[b] (mean ± SE)
Esophagus	0/1 (0%)	0 ± 0
Lung	0/2 (0%)	0 ± 0
Breast	0/1 (0%)	0 ± 0
Uterus	0/1 (0%)	0 ± 0
Colorectum	2/10 (20.0%)	0.565 ± 0.380
Liver	1/4 (25.0%)	0.174 ± 0.174
Pancreas	4/4 (100%)	15.220 ± 11.220
Papilla vater	1/1 (100%)	4.145 ± 0
Bile duct	3/5 (60.0%)	2.994 ± 1.950

[a] The amounts of α4GnT mRNA more than 40 copies/ml in a reaction tube are defined as positive.

[b] α4GnT:GAPDH mRNA ratios multiplied by 1.0×10^7 are indicated.

mononuclear cell fraction of peripheral blood isolated from patients with gastric cancer but not from healthy volunteers, and the expression level of α4GnT transcripts was increased in association with tumor progression, including tumor stage, depth of the tumor invasion, vessel invasion, and metastases. By combining the results obtained by immunohistochemistry and real-time RT-PCR, we also demonstrated that the expression level of α4GnT mRNA in the peripheral blood is clearly associated with the expression of α4GnT protein in gastric cancer cells (see Fig. 4). Moreover, it was also shown that α4GnT mRNA disappears from peripheral blood after the surgical removal of gastric cancer (see Table 2). Although the circulating tumor cells have not been identified directly in this study, these combined results strongly suggest that α4GnT mRNA detected in peripheral blood of the patients with gastric cancer originated from the circulating cancer cells. It would be a challenge to identify a small number of the circulating tumor cells in the peripheral blood by using morphological techniques such as immunocytochemistry using anti-α4GnT antibody or HIK1083 antibody directed to the GlcNAcα1→Galβ→R residue.

Among the serum tumor markers, CEA and CA19-9 are most widely used for the screening and monitoring of gastric cancer (Pectasides et al, 1997). However, these biomarkers have limitation for early detection of gastric cancer, because both markers tend to be elevated in advanced cancers than in early stages of the cancers. In fact, the present study revealed that in 19 patients with stage I gastric cancer, CEA was elevated only in 15.8% of the patients, and no patients were positive for CA19-9 (see Table 3). By contrast, the transcripts of α4GnT were detected in 57.9% of the same 19 patients with stage I gastric cancer. These results indicate that for early detection of gastric cancer, the real-time RT-PCR assay targeted to the α4GnT mRNA is much more sensitive than the immunoassay for CEA or CA19-9. CA72-4 is a tumor assay that detects the sialyl Tn antigen NeuAcα2→6GalNAcα1→Ser/Thr (Guadagni et al, 1996).

Immunohistochemical studies demonstrated that this carbohydrate antigen is highly expressed in gastric cancer cells (David et al, 1992; Victorzon et al, 1996). However, Kodama et al (1995) reported that the positive rates of CA72-4 in the sera of 100 patients with gastric cancer are 2.3% in early stage and 37.5% in the advanced stage. Future studies will be of significance to compare the clinical utility of α4GnT mRNA with CA72-4.

Extensive studies have been carried out to detect circulating tumor cells using RT-PCR method targeted to tissue- or epithelial cell–specific molecules such as CEA and CK19 for gastric cancer (Aihara et al, 1997; Majima et al, 2000; Nishida et al, 2000; Piva et al, 2000; Yeh et al, 1998), CEA and mutated *p53* gene for colorectal cancer (Guadagni et al, 2001; Jonas et al, 1996; Khan et al, 2000; Piva et al, 2000), human tissue kallikrein 2 for prostatic cancer (Kawakami et al, 1997), uroplakin II for urothelial cancer (Lu et al, 2000), and GM2/GD2 synthase for neuroblastoma (Hoon et al, 2001). Most of these studies demonstrated that the molecular detection by RT-PCR is feasible for the identification of circulating tumor cells in the peripheral blood. However, these assays were based on the ordinary RT-PCR method and thus did not accurately quantify the targeted molecules. By contrast, the recently introduced real-time RT-PCR technology made it possible to quantitatively analyze the circulating cancer cells using tissue-specific molecules such as prostate-specific antigen for prostate cancer (Straub et al, 2001) and MUC1 mucin for breast cancer (de Cremoux et al, 2000).

For gastric cancer, it was shown that gastric gland mucous cell–type mucins that have GlcNAcα1→Galβ→R residues formed by α4GnT are frequently expressed in the tumor cells but not in peripheral blood cells (Nakamura et al, 1998). In the present study, we thus chose α4GnT mRNA as a tissue-specific molecule of gastric cancer for the real-time RT-PCR assay. Absence of α4GnT mRNA in the peripheral blood cells was further verified using the blood cell cDNA panels. In addition to the gastric cancer, the gastric gland mucous cell–type mucin is shown to be frequently expressed in cancer cells derived from pancreas and biliary tract (Nakamura et al, 1998), suggesting that the real-time RT-PCR assay targeted to α4GnT would be useful for the detection of the pancreaticobiliary tract cancer. In fact, we found that significant amounts of the α4GnT mRNA can be detected in the peripheral blood isolated from the patients with pancreatic cancer, papilla vater cancer, and biliary tract cancer (see Table 4).

It was demonstrated that the real-time RT-PCR assay used in this study could detect α4GnT mRNA in as low as 40 copies/ml in a reaction tube. On the basis of this result, the minimum copy numbers of α4GnT mRNA in the peripheral blood detectable for this assay were calculated to be more than 1.6 copies in 5 ml of the peripheral blood containing approximately 2.0×10^7 to 5.0×10^7 mononuclear blood cells. Because the actual copy numbers of α4GnT mRNA in gastric cancer cells seem to be variable, it is difficult to estimate the minimum numbers of the cancer cells detected for this assay. However the frequent detection of α4GnT mRNA in the mononuclear cell fraction of the peripheral blood of the patients with stage I gastric cancer suggests that the gastric cancer cells expressing α4GnT mRNA are actually circulating in peripheral blood even in early stages of gastric cancer. Because the E- and/or P-selectin–mediated cell adhesion of cancer cells to the endothelial cells in remote organs is one of the critical events for metastatic colonization of the cancer cells (Fukuda, 1996; Hakomori, 1996; Nicolson, 1988), the detection of circulating cancer cells does not necessarily indicate the presence of metastasis. However, as shown in this study, the detection of circulating cancer cells in early stages of the gastric cancer indicates that (micro)metastases could already be occurring in the patients when the gastric cancer cells are still limited to the gastric mucosa or submucosa. In fact, Seto et al (2001) reported that the frequency of lymph node metastases of early gastric cancer is merely 8.9%. In addition, the strong correlation between the expression level of α4GnT mRNA and clinicopathological variables including the tumor stage suggests that more cancer cells are released to the blood stream when gastric cancer advances.

In the present study, the expression level of α4GnT mRNA in the mononuclear cell fraction of peripheral blood from the patients with *H. pylori*–infected chronic active gastritis and peptic gastroduodenal ulcer was also evaluated. Three of nine patients with chronic active gastritis and all of four patients with peptic gastroduodenal ulcer were actually positive for this assay. Although the significant difference was not obtained between the patients with gastric cancer and patients with these benign gastric disorders, mean value of α4GnT mRNA detected in chronic active gastritis and peptic gastroduodenal ulcer was lower than that in gastric cancer (see Fig. 3). By contrast, we have also shown that α4GnT mRNA was not detectable in the mononuclear cell fraction of peripheral blood isolated from healthy individuals. These combined results suggest that gastric gland mucous cells expressing α4GnT are not released into the peripheral blood under the normal conditions. However, once the mucosal disruption such as inflammation and ulceration occurs in gastric mucosa, the gastric gland mucous cells enter the blood stream through the injured sites. These results are consistent with our previous report that extensive biopsy of the gastric mucosa allows the gastric epithelial cells to enter the peripheral blood (Shimizu et al, 2000). Thus, detection of α4GnT mRNA in peripheral blood does not always exclude the possibility of benign mucosal injuries including chronic active gastritis and peptic gastroduodenal ulcer. However, this assay is noninvasive and sensitive enough for the early detection of gastric cancer compared with other ordinary tumor markers such as CEA and CA19-9. Therefore, we conclude that the real-time RT-PCR targeted to α4GnT mRNA will be useful for the screening of gastric cancer.

Materials and Methods

Patients and Samples

The present study involved 37 patients with gastric cancer (23 men and 14 women; age ranges, 46–97 years) and 29 patients with cancer other than gastric cancer (18 men and 11 women; age ranges, 40–81 years) including 10 cases of colorectal cancer; 5 cases of bile duct cancer; 4 cases of pancreatic cancer; 4 cases of hepatoma; 2 cases of lung cancer; and 1 case each of esophageal cancer, papilla vater cancer, breast cancer, and uterine cancer. These patients except for one with advanced gastric cancer with peritoneal dissemination subsequently underwent surgical operation for the removal of primary tumor at Shinshu University Hospital, Matsumoto, Japan, within 4 weeks in average after the diagnosis was established. In addition, 9 patients (7 males and 2 females; age ranges, 30–58 years) with *H. pylori*–infected chronic active gastritis, 4 patients (2 men and 2 women; age ranges, 66–83) with peptic gastroduodenal ulcer, and 23 healthy volunteers (14 men and 9 women; age ranges, 23–57 years) were enrolled in this study. Status of *H. pylori* infection was serologically determined using a PirikaplateG Helicobacter kit (Fujirebio, Tokyo, Japan) as described previously (Misawa et al, 1998), and the healthy volunteers, negative for *H. pylori* infection, were chosen. Histopathology of gastric cancer was evaluated on the basis of the Laurén (1965) classification, and tumor stage was categorized according to the histological tumor-node-metastasis classification system (Hayashi et al, 2000).

The peripheral blood samples were taken from these patients as well as healthy volunteers. In the patients with cancer, the blood samples were collected before surgical resection of the primary tumor, but the samples during postsurgical follow-up were also collected in three of the patients with gastric cancer. When the patients underwent endoscopic biopsy of the gastric mucosa, the blood samples were taken at least 2 weeks after the biopsy. In addition, human QUICK-Clone cDNA of leukocytes pooled from 550 male/female white individuals as well as human blood fractions multiple tissue cDNA (MTC) panel of the first-strand cDNA prepared from T cells, B cells, and monocytes were purchased from Clontech (Palo Alto, California). The MTC panel is composed of mononuclear cells (B cells, T cells, and monocytes) pooled from 50 male/female white individuals, resting CD8+ cells pooled from 33 male/female white individuals, resting CD4+ cells pooled from 20 male/female white individuals, resting CD14+ cells pooled from 36 male/female white individuals, resting CD19+ cells pooled from 34 male/female white individuals, CD19+ cells activated with pokeweed mitogen pooled from 4 male/female white individuals, mononuclear cells activated with pokeweed mitogen and concanavalin A pooled from 4 male/female white individuals, CD4+ cells activated with concanavalin A pooled from 12 male/female white individuals, and CD8 cells activated with PHA pooled from 8 male/female white individuals.

These samples were analyzed by a real-time quantitative RT-PCR assay. This study was approved by the institutional review board of the Shinshu University School of Medicine, Matsumoto, Japan, and written informed consent was obtained from all of the patients and healthy volunteers at Shinshu University Hospital before the study.

Immunohistochemisty for α4GnT

For detecting α4GnT in the gastric cancer cells, 29 gastrectomies for gastric cancer were further subjected to immunohistochemistry with monospecific anti-α4GnT polyclonal antibodies I17K using a Super Sensitive detection kit (BioGenex Laboratories, San Romon, California) as described previously (Zhang et al, 2001). Briefly, deparaffinized tissue sections sliced into 3-μm thickness were treated with 0.3% H_2O_2 in methanol and then blocked with 1% normal goat serum in Tris-buffered saline. The sections were incubated with I17K antibody for 1.5 hours. After the sections were washed with Tris-buffered saline, they were incubated with biotinylated anti-rabbit IgG and then horseradish peroxidase–labeled streptavidin. The peroxidase reaction was developed with a diaminobenzidine/H_2O_2 solution, and counterstaining was performed with hematoxylin. In control experiments performed by replacing the primary antibody with preimmune serum or omitting the primary antibody from the staining procedure, no specific staining was found. Tissue specimens containing more than 5% positively stained cancer cells were defined as positive, and others were classified as negative according to the criteria as described before (Machida et al, 2001).

RNA Extraction and cDNA Synthesis

Five milliliters of the peripheral blood anticoagulated with EDTA was collected and layered on 3 ml of Lymphprep (Nycomed Pharma, Oslo, Norway) in a 15-ml polypropylene tube. The tube was centrifuged at 2000 ×*g* for 30 minutes at 20°C. The mononuclear cell fraction was transferred to a new tube, resuspended in 5 ml of phosphate-buffered saline, and then centrifuged at 3000 ×*g* for 5 minutes. Total RNA was isolated from the pellet according to the acid guanidine thiocyanate-chloroform extraction method (Chomczynski and Sacchi, 1987) using ISOGEN-LS (Nippon Gene, Tokyo, Japan) and then incubated with 20 μl of a DNase I solution containing RNase inhibitor (Promega, Madison, Wisconsin) at 37°C for 10 minutes.

After inactivation of the DNase I by heating, reverse transcription of the total RNA extracted from the peripheral blood was performed in a final volume of 20 μl containing 10 μl of the DNase I–treated RNA, 2 μl of 5 × first strand buffer, 2 μl of 2 mM dNTPs, 0.2 μl of 0.1 M dithiothreitol, 1 μl of RNase inhibitor (Promega), 0.5 μl of M-MLV (Life Technologies, Gaithersburg, Maryland), and 1 μl of 0.5 mg/ml oligo$(dT)_{15}$ primer (Promega) at 42°C for 60 minutes. These samples

were kept at −80°C until the real-time quantitative RT-PCR analysis.

Real-Time Quantitative RT-PCR

The quantitation of α4GnT mRNA levels in the peripheral blood taken from the patients as well as healthy volunteers was performed using an ABI PRISM 7700 Sequence Detection System (PE Applied Biosystems, Foster City, California) based on the continuous optical monitoring of the progress of a fluorogenic PCR (Heid et al, 1996). In addition, the human blood cell cDNA panels including leukocytes, T cells, B cells, and monocytes purchased from Clontech were subjected to this assay. On the basis of the published sequence of human α4GnT (Nakayama et al, 1999), specific primer pair and probe were designed with the aid of the Primer Express program (PE Applied Biosystems). Forward and reverse primers for human α4GnT were 5'-GTTTTCCTCTTCCCTTTGGATATGA-3' (nucleotides 340 to 364), and 5'-TGCCACCGTATTTCCAGATGA-3' (nucleotides 490 to 470), respectively. These primers hybridized to different exons of the α4GnT gene. The TaqMan probe spanning the exon-exon junction was synthesized to be 5'-ACAATCAAATCAACGCCAGCGCAGA-3' (nucleotides 401 to 425) by PE Applied Biosystems, and it carried 5'-FAM (6-carboxyfluorescein) reporter label and 3'-TAMURA (6-carboxy-N,N,N',N'-tetramethylrhodamine) quencher group. A relative standard curve representing 10-fold dilutions of a human α4GnT cDNA (pcDNAI-α4GnT) ranging from 6×10^{-2} to 6×10^{-11} μg/ml was used for linear regression analysis of the patients' samples. PCR was carried out in 50 μl of reaction mixture containing 3 μl of the reverse transcription reaction, 1× Universal PCR Master Mix (PE Applied Biosystems), 900 nM of each primer, and 250 nM of the TaqMan probe.

For normalizing the expression level of α4GnT mRNA, GAPDH was also quantitatively analyzed in the same reactions. Thus, a partial cDNA of GAPDH was amplified from peripheral blood cells using a specific primer set for GAPDH (PE Applied Biosystems) and then subcloned into pCR2.1 (Invitrogen, San Diego, California). Ten-fold dilutions of the resultant vector, pCR2.1-GAPDH ranging from 1.2×10^{-2} to 1.2×10^{-6} μg/ml, were used to construct a relative standard curve for GAPDH. The PCR mixture was basically the same as that of α4GnT except for 200 nM GAPDH-specific TaqMan probe carrying 5'-VIC reporter label and 3'-TAMURA quencher group, and 500 nM of the specific primer for GAPDH purchased from PE Applied Biosystems.

These samples were placed in the ABI PRISM 7700 Sequence Analyzer and preheated at 95°C for 10 minutes, amplified for 50 cycles of 95°C for 15 seconds, followed by 60°C for 1 minute. The relative expression level of α4GnT was defined by multiplying α4GnT:GAPDH mRNA ratios by 1.0×10^{7}. The assays were performed in duplicate, and mean values of the two experiments were indicated.

Enzyme Immunoassay of CEA and CA19-9 in Patients' Serum

Expression levels of CEA in serum obtained from the 37 patients with gastric cancer before surgery were evaluated by enzyme immunoassay using CEA · Dainapack kit (Dainabot, Tokyo, Japan) with 2.5 ng/ml for cut-off value. In parallel, serum level of CA19–9 was also examined using an AxSYM CA19–9 · Dainapack kit (Dainabot) with 37 U/ml for cutoff value.

Statistical Analysis

Statistical analyses of the comparison between two independent groups were carried out using by Mann-Whitney *U* test. Similarly, the comparison among more than three groups was performed by use of Kruskal-Wallis test, followed by Dunnett's test. All of the statistical analyses were performed using StatVeiw 5.0 software (Abacus Concepts, Berkeley, California), and P values < 0.05 were considered to be statistically significant.

Acknowledgements

We thank Drs. Kosei Nakajima, Kazuyoshi Yamauchi, and Eiko Hidaka for valuable discussion during this study, Drs. Kazuhiko Ishihara and Kyoko Hotta for the generous gift of HIK1083 antibody, and Dr. Edgar Ong for critical reading of the manuscript.

References

Aihara T, Noguchi S, Ishikawa O, Furukawa H, Hiratsuka M, Ohigashi H, Nakamori S, Monden M, and Imaoka S (1997). Detection of pancreatic and gastric cancer cells in peripheral and portal blood by amplification of keratin 19 mRNA with reverse transcriptase-polymerase chain reaction. Int J Cancer 72:408–411.

Boku T, Nakane Y, Minoura T, Takada H, Yamamura M, Hioki K, and Yamamoto M (1990). Prognostic significance of serosal invasion and free intraperitoneal cancer cells in gastric cancer. Br J Surg 77:436–439.

Chomczynski P and Sacchi N (1987). Single-step method of RNA isolation by acid guanidinium thiocyanate-phenol-chloroform extraction. Anal Biochem 162:156–159.

David L, Nesland JM, Clausen H, Carneiro F, and Sobrinho-Simoes M (1992). Simple mucin-type carbohydrate antigens (Tn, sialosyl-Tn and T) in gastric mucosa, carcinomas and metastases. APMIS Suppl 27:162–172.

de Cremoux P, Extra JM, Denis MG, Pierga JY, Bourstyn E, Nos C, Clough KB, Boudou E, Martin EC, Muller A, Pouillart P, and Magdelenat H (2000). Detection of MUC1-expressing mammary carcinoma cells in the peripheral blood of breast cancer patients by real-time polymerase chain reaction. Clin Cancer Res 6:3117–3122.

Fukuda M (1996). Possible roles of tumor-associated carbohydrate antigens. Cancer Res 56:2237–2244.

Guadagni F, Kantor J, Aloe S, Carone MD, Spila A, D'Alessandro R, Abbolito MR, Cosimelli M, Graziano F, Carboni F, Carlini S, Perri P, Sciarretta F, Greiner JW, Kashmiri SV, Steinberg SM, Roselli M, and Schlom J (2001). Detection of blood-borne cells in colorectal cancer patients

by nested reverse transcription-polymerase chain reaction for carcinoembryonic antigen messenger RNA: Longitudinal analyses and demonstration of its potential importance as an adjunct to multiple serum markers. Cancer Res 61:2523–2532.

Guadagni F, Roselli M, Cosimelli M, Spila A, Cavaliere F, Tedesco M, Arcuri R, Abbolito MR, Casale V, Pericoli MN, Vecchione A, Casciani CU, Greiner JW, and Schlom J (1996). Correlation between tumor-associated glycoprotein 72 mucin levels in tumor and serum of colorectal patients as measured by the quantitative CA 72-4 immunoassay. Cancer Res 56:5293–5298.

Hakomori S (1996). Tumor malignancy defined by aberrant glycosylation and sphingo(glyco)lipid metabolism. Cancer Res 56:5309–5318.

Hayashi H, Ochiai T, Suzuki T, Shimada H, Hori S, Takeda A, and Miyazawa Y (2000). Superiority of a new UICC-TNM staging system for gastric carcinoma. Surgery 127:129–135.

Heid CA, Stevens J, Livak KJ, and Williams PM (1996). Real time quantitative PCR. Genome Res 6:986–994.

Hoon DS, Kuo CT, Wen S, Wang H, Metelitsa L, Reynolds CP, and Seeger RC (2001). Ganglioside GM2/GD2 synthetase mRNA is a marker for detection of infrequent neuroblastoma cells in bone marrow. Am J Pathol 159:493–500.

Ishihara K, Kurihara M, Goso Y, Urata T, Ota H, Katsuyama T, and Hotta K (1996). Peripheral α-linked N-acetylglucosamine on the carbohydrate moiety of mucin derived from mammalian gastric gland mucous cells: Epitope recognized by a newly characterized monoclonal antibody. Biochem J 318: 409–416.

Jonas S, Windeatt S, O-Boateng A, Fordy C, and Allen-Mersh TG (1996). Identification of carcinoembryonic antigen-producing cells circulating in the blood of patients with colorectal carcinoma by reverse transcriptase polymerase chain reaction. Gut 39:717–721.

Jung R, Kruger W, Hosch S, Holweg M, Kroger N, Gutensohn K, Wagener C, Neumaier M, and Zander AR (1998). Specificity of reverse transcriptase polymerase chain reaction assays designed for the detection of circulating cancer cells is influenced by cytokines in vivo and in vitro. Br J Cancer 78:1194–1198.

Kawakami M, Okaneya T, Furihata K, Nishizawa O, and Katsuyama T (1997). Detection of prostate cancer cells circulating in peripheral blood by reverse transcription-PCR for hKLK2. Cancer Res 57:4167–4170.

Khan ZA, Jonas SK, Le-Marer N, Patel H, Wharton RQ, Tarragona A, Ivison A, and Allen-Mersh TG (2000). p53 mutations in primary and metastatic tumors and circulating tumor cells from colorectal carcinoma patients. Clin Cancer Res 6:3499–3504.

Kodama I, Koufuji K, Kawabata S, Tetsu S, Tsuji Y, Takeda J, and Kakegawa T (1995). The clinical efficacy of CA 72-4 as serum marker for gastric cancer in comparison with CA19-9 and CEA. Int Surg 80:45–48.

Laurén T (1965). The two histologic main types of gastric carcinoma. Acta Pathol Microbiol Scand 64:34.

Lu JJ, Kakehi Y, Takahashi T, Wu XX, Yuasa T, Yoshiki T, Okada Y, Terachi T, and Ogawa O (2000). Detection of circulating cancer cells by reverse transcription-polymerase chain reaction for uroplakin II in peripheral blood of patients with urothelial cancer. Clin Cancer Res 6:3166–3171.

Machida E, Nakayama J, Amano J, and Fukuda M (2001). Clinicopathological significance of core 2 β1,6-N-acetylglucosaminyltransferase messenger RNA expressed in the pulmonary adenocarcinoma determined by in situ hybridization. Cancer Res 61:2226–2231.

Majima T, Ichikura T, Takayama E, Chochi K, and Mochizuki H (2000). Detecting circulating cancer cells using reverse transcriptase-polymerase chain reaction for cytokeratin mRNA in peripheral blood from patients with gastric cancer. Jpn J Clin Oncol 30:499–503.

Misawa K, Kumagai T, Shimizu T, Furihata K, Ota H, Akamatsu T, and Katsuyama T (1998). A new histological procedure for re-evaluation of the serological test for Helicobacter pylori. Eur J Clin Microbiol Infect Dis 17:14–19.

Nakamura N, Ota H, Katsuyama T, Akamatsu T, Ishihara K, Kurihara M, and Hotta K (1998). Histochemical reactivity of normal, metaplastic, and neoplastic tissues to α-linked N-acetylglucosamine residue-specific monoclonal antibody HIK1083. J Histochem Cytochem 46:793–801.

Nakayama J (2002). α4-N-acetylglucosaminyltransferase. In: Taniguchi N, Honke K, and Fukuda M, editors. Handbook of glycosyltransferases and related genes. Tokyo: Springer-Verlag, 151–157.

Nakayama J, Yeh J-C, Misra AK, Ito S, Katsuyama T, and Fukuda M (1999). Expression cloning of a human α1, 4-N-acetylglucosaminyltransferase that forms GlcNAcα1→4Galβ→R, a glycan specifically expressed in the gastric gland mucous cell-type mucin. Proc Natl Acad Sci USA 96:8991–8996.

Nicolson GL (1988). Cancer metastasis: Tumor cell and host organ properties important in metastasis to specific secondary sites. Biochim Biophys Acta 948:175–224.

Nishida S, Kitamura K, Ichikawa D, Koike H, Tani N, and Yamagishi H (2000). Molecular detection of disseminated cancer cells in the peripheral blood of patients with gastric cancer. Anticancer Res 20:2155–2159.

Patino JF (1994). The current management of gastric cancer. Adv Surg 27:1–19.

Pectasides D, Mylonakis A, Kostopoulou M, Papadopoulou M, Triantafillis D, Varthalitis J, Dimitriades M, and Athanassiou A (1997). CEA, CA 19-9, and CA-50 in monitoring gastric carcinoma. Am J Clin Oncol 20:348–353.

Piva MG, Navaglia F, Basso D, Fogar P, Roveroni G, Gallo N, Zambon CF, Pedrazzoli S, and Plebani M (2000). CEA mRNA identification in peripheral blood is feasible for colorectal, but not for gastric or pancreatic cancer staging. Oncology 59: 323–328.

Seto Y, Shimoyama S, Kitayama J, Mafune K, Kaminishi M, Aikou T, Arai K, Ohta K, Nashimoto A, Honda I, Yamagishi H, and Yamamura Y (2001). Lymph node metastasis and preoperative diagnosis of depth of invasion in early gastric cancer. Gastric Cancer 4:34–38.

Shimizu F, Nakayama J, Sugiyama A, Kawasaki S, and Katsuyama T (2000). Gastric gland mucous cells circulate in peripheral blood after endoscopic biopsy of the gastric mucosa. Am J Gastroenterol 95:3017–3018.

Straub B, Muller M, Krause H, Schrader M, Goessl C, Heicappell R, and Miller K (2001). Detection of prostate-specific antigen RNA before and after radical retropubic prostatectomy and transurethral resection of the prostate

using "Light-Cycler"-based quantitative real-time polymerase chain reaction. Urology 58:815–820.

Sun J, Misumi J, Shimaoka A, Aoki K, and Esaki F (2001). Stomach cancer-related mortality. Eur J Cancer Prev 10:61–66.

Victorzon M, Nordling S, Nilsson O, Roberts PJ, and Haglund C (1996). Sialyl Tn antigen is an independent predictor of outcome in patients with gastric cancer. Int J Cancer 65:295–300.

Wanebo HJ, Kennedy BJ, Chmiel J, Steele G Jr, Winchester D, and Osteen R (1993). Cancer of the stomach. A patient care study by the American College of Surgeons. Ann Surg 218:583–592.

Yeh KH, Chen YC, Yeh SH, Chen CP, Lin JT, and Cheng AL (1998). Detection of circulating cancer cells by nested reverse transcription-polymerase chain reaction of cytokeratin-19 (K19): Possible clinical significance in advanced gastric cancer. Anticancer Res 18:1283–1286.

Zhang MX, Nakayama J, Hidaka E, Kubota S, Yan J, Ota H, and Fukuda M (2001). Immunohistochemical demonstration of α1,4-N-acetylglucosaminyltransferase that forms GlcNAcα1,4Galβ residues in human gastrointestinal mucosa. J Histochem Cytochem 49:587–596.

American Journal of Pathology, Vol. 163, No. 6, December 2003

Implantation-Dependent Expression of Trophinin by Maternal Fallopian Tube Epithelia during Tubal Pregnancies

Possible Role of Human Chorionic Gonadotrophin on Ectopic Pregnancy

Jun Nakayama,* Daisuke Aoki,† Tomoaki Suga,‡ Tomoya O. Akama,§ Satoshi Ishizone,¶ Hirohito Yamaguchi,‖ Kazuhiko Imakawa,‖ Daita Nadano,** Asgerally T. Fazleabas,†† Tsutomu Katsuyama,‡‡ Shiro Nozawa,† and Michiko N. Fukuda§

From the Departments of Pathology, Internal Medicine,‡ Surgery,¶ and Laboratory Medicine,‡‡ Shinshu University School of Medicine, Matsumoto, Japan; the Department of Obstetrics and Gynecology,† School of Medicine, Keio University, Tokyo, Japan; the Laboratory of Animal Breeding,‖ University of Tokyo, Tokyo, Japan; the Department of Applied Molecular Biosciences,** Graduate School of Bioagricultural Sciences, Nagoya University, Nagoya, Japan; the Department of Obstetrics and Gynecology,†† University of Illinois, Chicago, Illinois; and the Glycobiology Program,§ The Burnham Institute, La Jolla, California*

Trophinin, tastin, and bystin have been identified as molecules potentially involved in human embryo implantation. Both trophoblasts and endometrial epithelial cells express trophinin, which mediates apical cell adhesion through homophilic trophinin-trophinin binding. We hypothesized that trophinin's function in embryo implantation is unique to humans and investigated the expression of trophinin, tastin, and bystin in ectopic pregnancy, a condition unique to humans. In tubal pregnancies, high levels of all three were found in both trophoblasts and fallopian tubal epithelia. Trophinin expression in maternal cells was particularly high in the area adjacent to the trophoblasts, whereas trophinin was barely detectable in intact fallopian tubes from women with *in utero* pregnancies or without pregnancies. When explants of intact fallopian tube were incubated with the human chorionic gonadotrophin (hCG), trophinin expression was enhanced in epithelial cells. Since the trophectoderm of the human blastocyst secretes hCG before and after implantation, these results suggest that hCG from the human embryo induces trophinin expression by maternal cells. As both β-subunit of hCG and trophinin genes have diverged in mammals, the present study suggests a unique role of hCG and trophinin in human embryo implantation, including the pathogenesis of ectopic pregnancy. *(Am J Pathol 2003, 163:2211–2219)*

Ectopic pregnancy occurs at a rate of 0.25 to 1.4% in all pregnancies in humans, and over 95% of all ectopic pregnancies occur in the fallopian tube.[1,2] Extrauterine implantation does not occur naturally or experimentally in other animals including non-human primates.[3–5] It is not known why extrauterine implantation occurs only in humans.

The human embryo enters the uterine cavity 4 days after ovulation.[6] Blastocyst implantation takes place around day 7 after ovulation. During this period, the endometrial luminal epithelium becomes receptive to blastocyst adhesion in response to rising serum progesterone and peptide hormones from the newly formed corpus luteum, opening an implantation window.[7,8]

The blastocyst free from the *zona pellucida* is sticky *in vitro*. Human trophoblastic cells avidly bind to fibronectin, laminin, and type IV and V collagen,[9] all of which are present in decidualized endometrial stroma. Therefore, injuries to the epithelium that expose this underlying matrix can enable trophoblast elements to adhere and grow, potentially causing ectopic pregnancy. The receptive human endometrium expresses α_V/β_3 integrin on the apical surfaces of the luminal epithelium.[8] This integrin type is

Supported by NIH grant HD34108 and grant from Kyowa Medex (to M.N.F.), NIH grant HD29964 (to A.T.F.), Grant-in-Aid for Scientific Research B-15390115 from the Japan Society for the Promotion of Science (to J.N.), and Keio University Special Grant-in-Aid for Innovative Collaborative Research Projects (to S.N.).

Accepted for publication August 11, 2003.

Address reprint requests to Jun Nakayama, Department of Pathology, Shinshu University School of Medicine, Matsumoto 390-8621, Japan, E-mail: jun@hsp.md.shinshu-u.ac.jp; or Michiko N. Fukuda, The Burnham Institute, 10901 North Torrey Pines Road, La Jolla, CA 92037. E-mail: michiko@burnham-inst.org.

Table 1. Expression of Trophinin, Tastin, and Bystin Proteins in the Fallopian Tube from Patients Unrelated to Tubal Pregnancy

Patient no.	Age	Menstrual cycle or gestational age (day)	Trophinin	Tastin	Bystin
1	24	proliferative phase	+*	+++	−
2	28	98 days pregnancy	−	++	+++
3	42	49 days pregnancy	+	+++	+++
4	19	secretory phase	−	+	−
5	19	secretory phase	−	++	++
6	48	secretory phase	+	++	++
7	47	proliferative phase	+	++	++
8	50	proliferative phase	−	++	+++
9	50	proliferative phase	−	+	++
10	40	44 days pregnancy	−	+++	+
11	37	proliferative phase	−	+	++

*−, +, ++, and +++ show no, minimal, moderate, and maximal immunohistochemical reactivity, respectively.

also found in the normal human fallopian tube epithelium, suggesting the existence of a tubal implantation window.[10] However, given that tubal pregnancy does not occur in animals, it is difficult to explain the mechanism of ectopic pregnancy by the activity of evolutionarily conserved molecules such as integrins.

Previously, we identified and characterized a novel molecular complex, composed of trophinin, tastin and bystin, mediating apical cell adhesion between human trophoblasts and endometrial epithelial cells.[11–17] Trophinin is an integral membrane protein, and part of this polypeptide is exposed on the cell surface. Tastin and bystin are cytoplasmic proteins required for trophinin to exhibit efficient cell adhesion activity. Trophoblastic cells and endometrial epithelial cells expressing these molecules adhere to each other at their respective apical plasma membranes. Human endometrium tightly regulates expression of trophinin, which is expressed only within a restricted region of the apical side of luminal endometrial epithelium at a time coincident with the "implantation window."[11] In the human placenta at early stages of pregnancy, trophinin, tastin and bystin are strongly expressed in the trophoblast of chorionic villi and in the endometrial glandular epithelium, particularly at the utero-placental interface.[15] Studies of mouse trophinin indicate significant differences from human trophinin in expression patterns and roles *in vivo*.[16,17] Trophinin is not found in mouse trophoblastic cells during and after implantation.[16,17] Trophinin null mutant mice show no defects in embryo implantation.[17] The *in vivo* role of human trophinin in embryo implantation remains to be proved.

We hypothesized that trophinin's function in embryo implantation is unique to humans. The present study was undertaken to evaluate this hypothesis by determining the expression pattern of trophinin in ectopic pregnancy, a condition unique to humans. Here we show that, in tubal pregnancies, trophinin is strongly expressed by both the embryonic trophoblasts and maternal fallopian tube epithelia. The expression pattern of trophinin suggests that a factor derived from the implanting embryo induces trophinin expression by maternal cells. We found that the human chorionic gonadotrophin (hCG) induces trophinin expression by epithelial cells in the fallopian tube, which was determined by quantitative RT-PCR for trophinin transcripts and immunohistochemistry for trophinin protein. Thus the results suggest strongly that trophinin and hCG together play unique roles in human embryo implantation, including the pathogenesis of ectopic pregnancies.

Materials and Methods

Tissue Collection

Twenty-three tissue blocks of fallopian tubes resected from 23 patients with ectopic tubal pregnancy were retrieved from the archives of Shinshu University Hospital and Keio University Hospital, Japan. In addition, paraffin blocks of intact fallopian tubes removed from 11 patients with benign uterine or ovarian diseases were also retrieved from the same archives. Three of these 11 patients were found to be associated with *in utero* pregnancy. All archival samples were obtained with informed consent. Age, gestational age, or menstrual cycle of the patients are listed in Tables 1 and 2. These specimens were fixed for 48 hours in 20% buffered formalin (pH 7.4), embedded in paraffin, and sectioned serially at 3-μm thickness for immunohistochemistry or at 7-μm thickness for *in situ* hybridization.

In parallel, four tissue specimens of fresh intact fallopian tubes were obtained from the patients who underwent hysterectomy for uterine diseases after informed consent was obtained at Keio University Hospital. All of the patients were cyclic women, and their ages ranged from 26 to 52 years. The fallopian tube specimens from two patients (26- and 43-years-old) were cut into small pieces and cultured at 37°C in a 5% CO_2 incubator in Ham's F-12 medium (Nissui Pharmaceutical Co, Tokyo, Japan) containing 10% fetal calf serum in the presence of 10 IU/ml or 100 IU/ml hCG (from pregnancy urine, Teikoku Hormone Mfg, Tokyo, Japan). As a control, hCG was omitted from the culture medium. On culturing for 6 and 24 hours, the explants were subjected to quantitative analysis of trophinin mRNA. On the other hand, the fallopian tube specimens from two patients (41- and 52-years-old) were cultured for 24 hours in the presence or absence of hCG in the similar manner as described above, and tissues were analyzed for trophinin protein by immunohistochemistry.

Table 2. Expression of Trophinin, Tastin, and Bystin Proteins in the Fallopian Tubes during Tubal Pregnancy

Patient no.	Age	Gestational age (day)	Trophinin	Tastin	Bystin
1	30	41	+++*	+++	+++
2	36	61	+++	++	+++
3	24	122	+++	+++	+++
4	37	73	+++	+++	+++
5	35	49	++	+++	++
6	29	56	+++	+++	+++
7	26	44	+++	+++	+++
8	35	50	++	++	++
9	37	51	+++	++	+++
10	25	50	+++	+++	+++
11	40	58	++	+++	++
12	30	48	+	+	++
13	36	55	+++	+++	+++
14	36	58	++	++	++
15	34	49	+++	++	++
16	29	56	+++	++	+
17	37	49	++	++	+++
18	22	47	+++	++	+++
19	31	52	++	+++	+++
20	34	43	++	+	+++
21	24	57	+++	+++	+++
22	29	71	+++	+++	+++
23	22	47	++	+++	++

*−, +, ++, and +++ show no, minimal, moderate, and maximal immunohistochemical reactivity, respectively.

Immunohistochemistry

The tissue specimens were fixed for 48 hours in 20% buffered formalin, embedded in paraffin, and sectioned serially at 3-μm thickness. Immunohistochemistry was performed by an indirect immunoperoxidase method using monoclonal antibodies specific for trophinin, bystin, and tastin, as described.[15] Briefly, tissue sections were immersed in absolute methanol containing 0.3% H_2O_2 for 30 minutes and then washed with PBS. For primary antibodies, monoclonal anti-trophinin (clone 3–11, mouse IgM), anti-bystin (clone 19, mouse IgM), or anti-tastin (clone 38, mouse IgM) antibodies were used, and for the secondary antibody, goat anti-mouse Ig conjugated with horseradish peroxidase (DAKO, Carpinteria, CA) was used. Peroxidase activity was visualized with a diaminobenzidine-hydrogen peroxide solution. Similarly, immunohistochemistry for hCG was performed using polyclonal anti-hCG antibodies (DAKO) and anti-rabbit Ig conjugated with horseradish peroxidase (DAKO) as a secondary antibody. Control experiments were carried out either by omitting the primary antibodies or using an irrelevant isotype-matched primary antibody; ie, HIK1083 (Kanto Kagaku, Tokyo, Japan) specific for GlcNAcα1→4Galβ→R.[18] No specific signal was noted in these control experiments.

In Situ *Hybridization*

To detect trophinin, tastin, and bystin transcripts, *in situ* hybridization was carried out using RNA probes specific for these molecules, as described previously.[15,19] Briefly, digoxigenin-labeled anti-sense and sense probes were prepared by *in vitro* transcription from pGEM-3Zf(+) plasmids (Promega, Madison, WI) containing specific DNA fragments of trophinin (nucleotides −3 to +149; the first nucleotide of the initiation codon is defined as +1), tastin (−26 to +124), and bystin (+627 to +796). The deparaffinized tissue sections from tubal pregnancy and intact fallopian tubes were immersed in 0.2 mol/L HCl for 20 minutes, digested with 100 μg/ml proteinase K at 37°C for 20 minutes, and post-fixed with 4% paraformaldehyde. The slides were rinsed with 2 mg/ml glycine, acetylated for 10 minutes in 0.25% acetic anhydride in 0.1 mol/L triethanolamine (pH 8.0), defatted with chloroform, and air-dried. After prehybridization with 50% deionized formamide/2X SSC for 1 hour at 45°C, the slides were hybridized with 0.5 mg/ml of anti-sense or sense probe in 50% deionized formamide, 2.5 mmol/L EDTA (pH 8.0), 300 mmol/L NaCl, 1X Denhardt's solution, 10% dextran sulfate, and 1 mg/ml brewer's yeast tRNA at 45°C for 48 hours. After hybridization, the slides were washed in 50% formamide/2X SSC for 1 hour at 45°C and digested with 10 mg/ml RNase A at 37°C for 30 minutes. After sequential washing with 2X SSC/50% formamide at 45°C for 1 hour and 1X SSC/50% formamide at 45°C for 1 hour, the sections were subjected to immunohistochemistry for detection of hybridized probes using an alkaline phosphatase-conjugated anti-digoxigenin antibody (Roche Molecular Biochemicals, Alameda, CA). Digoxigenin was detected by alkaline phosphatase by incubating with 5-bromo-4-chloro-3-indolyl phosphate and nitroblue tetrazolium in the presence of 0.2 mmol/L levamisole and 10% polyvinylalcohol for 30 minutes at room temperature. No specific signals were detected in the control experiments using sense probes.

Quantitative Analysis of Trophinin mRNA

The intact fallopian tubes obtained from two patients (26- and 43-years-old) on hysterectomy were cultured in the presence or absence of hCG for 6 hours and for 24 hours as described above. Total RNA was isolated from the tissue explants using Isogen (Nippon Gene, Tokyo, Japan). After digestion with DNase I, reverse transcription of the total RNA was performed in a final volume of 20 μl containing 4 μl of 5X first strand buffer, 2 μl of 2 mmol/L dNTPs, 0.2 μl of 0.1 mol/L DTT, 1 μl of RNase inhibitor, 0.5 μl of M-MLV reverse transcriptase, and 1 μl of oligo dT primer at 42°C for 60 minutes.

Quantitative analysis of trophinin mRNA expressed in the fallopian tubes was carried out using an ABI PRISM 7700 Sequence Detection System (PE Applied Biosystems, Foster City, CA). Specific primer pair and probe were designed with the aid of the Primer Express program (PE Applied Biosystems). Forward and reverse primers for human trophinin were 5′-AGGGAAGAGTTAGGCGATGATTC-3′ (nucleotides +22 to +44), and 5′-TTGGGCTCTGGCCTCAATT-3′ (nucleotides +72 to + 90), respectively. The TaqMan probe, 5′-CAAATGAAAATCTGCTCCAGGCCTG-3′ (nucleotides +46 to +70), which carries 5′-FAM (6-carboxyfluorescein) reporter label and 3′-TAMURA (6-carboxy-N, N, N′,

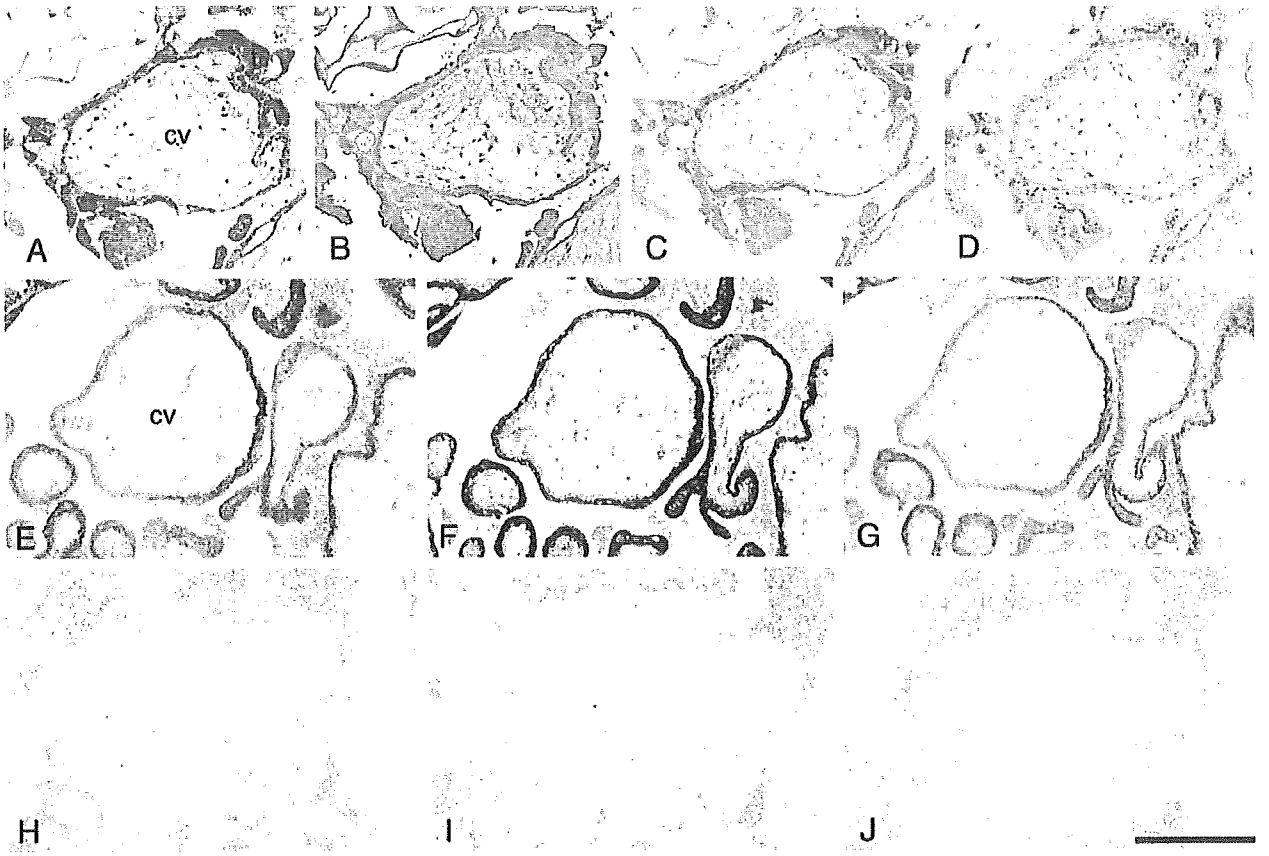

Figure 1. Expression of trophinin, tastin, and bystin proteins and their transcripts in the chorionic villi from tubal pregnancy. Immunohistochemistry for trophinin (**A**), tastin (**B**), bystin (**C**), second antibody alone (**D**), and *in situ* hybridization for trophinin (**E**, antisense; **H**, sense), tastin (**F**, antisense; **I**, sense), and bystin (**G**, antisense; **J**, sense) using digoxigenin-labeled RNA probes. All photographs presented are in the same magnification, and the **bar** in (**J**) indicates 200 μm. (cv, chorionic villi; t, trophoblasts).

N′-tetramethylrhodamine) quencher group was synthesized by PE Applied Biosystems. A relative standard curve representing tenfold dilutions of a trophinin cDNA (pcDNAI-trophinin[11]) ranging from 10^{10} to 10^{1} copies/ml was used for linear regression analysis for trophinin mRNA. A standard curve ranging from 10^{10} to 10^{1} copies/ml for a housekeeping gene, glyceraldehyde-3-phosphate dehydrogenase (GAPDH), was prepared in the same tube that trophinin cDNA was prepared, and this was used for normalizing the samples.[20]

Multiplex PCR was carried out in 50 μl of reaction mixture containing 3 μl of cDNA sample, 1X Universal PCR Master Mix (PE Applied Biosystems), 800 nmol/L of the primer pair for trophinin, 800 nmol/L of the primer pair for GAPDH, 200 nmol/L of the TaqMan probe for trophinin, and 200 nmol/L of the TaqMan probe for GAPDH that carries 5′-VIC reporter label and 3′-TAMURA quencher group (PE Applied Biosystems). These reaction tubes were placed in the ABI PRISM 7700 Sequence Analyzer, and preheated at 95°C for 10 minutes, followed by 50 cycles of denaturation at 95°C for 15 seconds and annealing/extension at 60°C for 1 minute. The quantity of trophinin mRNA was determined using the standard curve of trophinin cDNA on normalizing the sample size by GAPDH. The quantitity of trophinin mRNA was expressed as the relative amount of GAPDH mRNA, thus the ratio of trophinin mRNA to GAPDH multiplied by 100. The assays were performed in duplicate, and the mean values of the two experiments were indicated.

Results

Expression of Trophinin, Tastin, and Bystin by Trophoblasts of Chorionic Villi during Tubal Pregnancy

Immunohistochemistry of the fallopian tube from ectopic pregnancy patients using anti-hCG antibodies showed expression of hCG, a trophoblast marker, in the chorionic villous trophoblasts but not in the tubal epithelia (data not shown). Immunohistochemistry showed strong expression of trophinin, tastin, and bystin proteins in trophoblasts of the chorionic villi (Figure 1, A to C). These results were confirmed by *in situ* hybridization, demonstrating that transcripts of these molecules are strongly expressed in trophoblastic cells (Figure 1, E to G). The expression patterns of these proteins and transcripts are similar to those observed previously in the human placenta in normal pregnancy.[15]